UCRL-17007

University of California

Ernest O. Lawrence Radiation Laboratory

SIGN OF THE $K_1^0 - K_2^0$ MASS DIFFERENCE

Berkeley, California

Special Thesis

UCRL-17007

UNIVERSITY OF CALIFORNIA
Lawrence Radiation Laboratory
Berkeley, California

AEC Contract No. W-7405-eng-48

SIGN OF THE K_1^0 - K_2^0 MASS DIFFERENCE

Gerald Warren Meisner

(Ph. D. Thesis)

July 22, 1966

SIGN OF THE $K_1^0 - K_2^0$ MASS DIFFERENCE

Contents

SIGN OF THE K_1^0 - K_2^0 MASS DIFFERENCE

Gerald Warren Meisner

Lawrence Radiation Laboratory
University of California
Berkeley, California

July 22, 1966

ABSTRACT

We have performed an experiment to measure the sign of $m_1 - m_2$ by following the time development of $K_{neutral}$-p elastic scatters. We find K_2^0 to be heavier than K_1^0. Our statistical confidence level depends on the unresolved Fermi-Yang-type (F-Y) ambiguity that exists at present in the KN (strangeness S = +1) phase shifts in isotopic-spin state I = 0. If the F solution (large positive $p_{3/2}$ phase shift) is correct, we obtain Monte Carlo betting odds of 45 to 1 for $m_2 > m_1$, assuming $|m_1 - m_2| = 0.57\,\tau_1^{-1}$. If instead the Y solution (large positive $p_{1/2}$ phase shift) is correct, our betting odds for $m_2 > m_1$ are 5 to 1. We have not resolved the F-Y ambiguity.

I. INTRODUCTION

The magnitude of the K_1^0-K_2^0 mass difference, $|m_1 - m_2|$, has been established to be about $0.6\ \tau_1^{-1}$ (Ref. 1)($\approx 3\times10^{-6}$ eV/c^2 or $\approx 10^{-11}\ m_e$ or $\approx 10^{-38}$ grams!), with the assumption that $\tau_1 = 0.88\times10^{-10}$ sec. Few experiments have been designed to measure the sign of the difference, although several methods have been proposed.

Kobzarov and Okun' suggested measuring the K_1^0 amplitude regenerated by a K_2^0 beam passing through two regenerators of different materials separated by a fixed gap, and then reversing the relative position of the two slabs and repeating the measurements[2]; Jovanovich et al.[3] tried this method and found evidence that K_2^0 is heavier than K_1^0. A different method, utilizing interference effects between the final state of the original and regenerated K_1^0, was proposed by Piccioni et al.[4], who recently used the method and presented evidence that K_2^0 is heavier than K_1^0. A third method, and the one we used, was advanced by Camerini, Fry, and Gaidos.[5] In this method, one starts with neutral K's of known strangeness and detects the time development of elastic scatters followed by K_1^0 decays.[6] Since we performed our experiment in a hydrogen bubble chamber, we must rely on knowledge of elastic scattering amplitudes in the KN and $\overline{K}$N channels. Unfortunately, there is a Fermi-Yang-type ambiguity[7] in the KN phase shifts in isotopic-spin state I = 0 at the momentum of the kaons ($0 < P_K < 600$ MeV/c) used in this experiment. We discuss consequences of this ambiguity in Sec. IV.

In Sec. II we present some theoretical consequences of the K^0-$\overline{K}^0$ mixing scheme postulated by Gell-Mann and Pais[8]; in Sec. III we discuss the beam set-up, scanning procedures, and data processing; in Sec. IV we present results from the analysis of our data; and in Sec. V we discuss our conclusions.

II. THEORY

In 1955 Gell-Mann and Pais[8] postulated that the K^0 - $\overline{K}^0$ system was not to be thought of as two one-component systems; rather, the K^0 and $\overline{K}^0$ should be considered as two components of a single system. Thus, one should write the probability amplitude ψ_K of the neutral K system as a superposition of amplitudes of K^0 and $\overline{K}^0$, eigenstates of the strong-interaction Hamiltonian:

$$|\psi_K\rangle = a\,|K^0\rangle + b\,|\overline{K}^0\rangle$$

where $|a|^2$ and $|b|^2$ are the probabilities of observing a K^0 and a $\overline{K}^0$ respectively. Since the K^0 and $\overline{K}^0$ are each other's antiparticles, they must have identical masses and lifetimes.[9] However, experimenters have measured two distinct lifetimes[10] for the neutral K system and a distinct mass difference[1] between the two decay eigenstates. Labeling the two eigenstates K_1^0 and K_2^0, adopting a conventional choice of phase, and neglecting CP non-conservation,[5] we can write these decay eigenstates as linear combinations of the degenerate K^0 and $\overline{K}^0$:

$$|K_1^0\rangle = (|K^0\rangle + |\overline{K}^0\rangle)/\sqrt{2}\ , \quad |K_2^0\rangle = (|K^0\rangle - |\overline{K}^0\rangle)/\sqrt{2}. \tag{1}$$

Assuming that the time development of the decay eigenstates is governed[11] by the factor $\exp(-imt-\lambda t/2)$ in the particles rest frame, where m is the mass of the particle and λ is the decay rate, we can write the probability amplitude ψ_K for the neutral K system at time t, which at $t = 0$ was pure K^0, as

$$\sqrt{2}\,\psi_K = |K_1^0\rangle \exp(-im_1t-\lambda_1t/2) + |K_2^0\rangle \exp(-im_2t-\lambda_2t/2). \tag{2}$$

Using Eq. (2) and projecting out the K^0 and $\overline{K}^0$ components, we have their time-dependent amplitudes[12]:

$$2(K^0, \psi_K) = \exp(-im_1t-\lambda_1t/2) + \exp(-im_2t-\lambda_2t/2) \tag{3a}$$

$$2(\overline{K}^0, \psi_K) = \exp(-im_1t-\lambda_1t/2) - \exp(-im_2t-\lambda_2t/2). \tag{3b}$$

The absolute squares of Eq. (3) give the unnormalized counting rates of

K^0 and $\overline{K}^0$ interactions; these rates are a function of the magnitude of the mass difference. To get information on the sign of the mass difference, one can observe neutral K elastic scatters followed by a K_1 or K_2 decay. If A and $\overline{A}$ are amplitudes for elastic K^0-p and $\overline{K}^0$-p scattering, we can write the amplitude of the neutral K system immediately following an elastic scatter at time t as[12]

$$(2)^{3/2}\psi(t) = [(A+\overline{A})\,e^{-im_1t-\lambda_1t/2} + (A-\overline{A})\,e^{-im_2t-\lambda_2t/2}]\,K_1^0 + [(A-\overline{A})\,e^{-im_1t-\lambda_1t/2} + (A+\overline{A})\,e^{-im_2t-\lambda_2t/2}]\,K_2^0. \qquad (4)$$

If T' is the potential proper time of the K_1^0 from the position of the elastic scatter to the edge of the fiducial volume, the probability of their being an elastic scatter at time t followed by a K_1^0 decay within the fiducial volume is proportional to $[1 - \exp(-\lambda_1 T')]I_1$, where

$$I_1 = |A+\overline{A}|^2 \exp(-\lambda_1 t) + |A-\overline{A}|^2 \exp(-\lambda_2 t) + 2\exp[-\tfrac{1}{2}(\lambda_1+\lambda_2)t] \cdot \{(|A|^2-|\overline{A}|^2)\cos[(m_1-m_2)t] + 2\,\mathrm{Im}A^*\overline{A}\sin[(m_1-m_2)t]\}. \qquad (5)$$

This simple but daring application of the principle of superposition, a cornerstone of quantum mechanics, leads to unusual results, some of which are contained in Eqs. (3) and (5). For example, the absolute square of Eq. (3b) tells us that even though at $t = 0$ the probability of observing a $\overline{K}^0$ interaction is zero, at some later time the probability is finite and varies sinusoidally with a period inversely proportional to $|m_1-m_2|$.

Since there appear to be no ΔS(strangeness) = 2 transitions allowed, this increase and decrease of the K^0 and $\overline{K}^0$ amplitudes with time can take place only because there are intermediate states common to both particles, the dominant one being 2π. That is, K^0 and $\overline{K}^0$ both appear to decay into two pions with an equal rate (more precisely, the 2π decay rates from K^0 and $\overline{K}^0$ production are consistent with one another); therefore, since there must be some amplitude for the virtual process $2\pi \rightarrow K^0$, there exists the virtual process $K^0 \leftrightarrow 2\pi \leftrightarrow \bar{K}^0$, which can account for the transfer of probability between the two eigenstates.

The phenomenon of energy exchange in a coupled system is not unusual in physics. The transfer of energy between inductor and capacitor in an L-C circuit is a familiar example. A mechanical example, a model of which has been built and used by Professor Frank S. Crawford, Jr., for pedagogical purposes, consists of two pendula of equal length ℓ coupled by a spring, as is shown in Fig. 1(a). We discuss in some detail how a study of the coupled-pendula problem can help us understand the quantum-mechanical K^0-$\bar{K}^0$ problem.

We label the left pendulum K^0 and the right pendulum $\bar{K}^0$, and measure displacements from equilibrium as indicated. Since the lengths of the pendula are equal, the periods of oscillation will also be equal if there is no coupling spring. In our quantum mechanical analog, the K^0 and $\bar{K}^0$ have equal masses; a fortiori, their natural frequencies ω, given by the relation $\hbar\omega = mc^2$, will also be equal.

Finding the normal modes of the coupled pendula, that is, those motions which are entirely independent of one another and which will consequently not transfer energy back and forth, is a straightforward procedure and is handled in many textbooks on mechanics.[13] (In the language of quantum mechanics, we want to find the eigenfunctions of the K^0-$\bar{K}^0$ system.) By inspection, we can see that one independent motion consists of the pendula moving equal distances in opposite directions. This mode is shown in Fig. 1(b) where the total displacement $X = X^0 + \bar{X}^0 \equiv X_1$. This mode will die out with a lifetime characterized by the spring's inelasticity. The second independent mode, shown in Fig. 1(c), consists of the pendula moving in unison without disturbing the spring, so that the net displacement $X = X^0 - \bar{X}^0 \equiv X_2$. This mode will not damp out if we neglect friction from air and from pivots supporting the pendula. It is easy to show that the first mode has a frequency of oscillation $\omega_1 = \sqrt{(\ell/g)+(2k/m)}$, where g equals 32.16 ft/sec^2, k is the stiffness coefficient of the spring, and m is the mass of the pendula, and that the frequency of the second normal mode

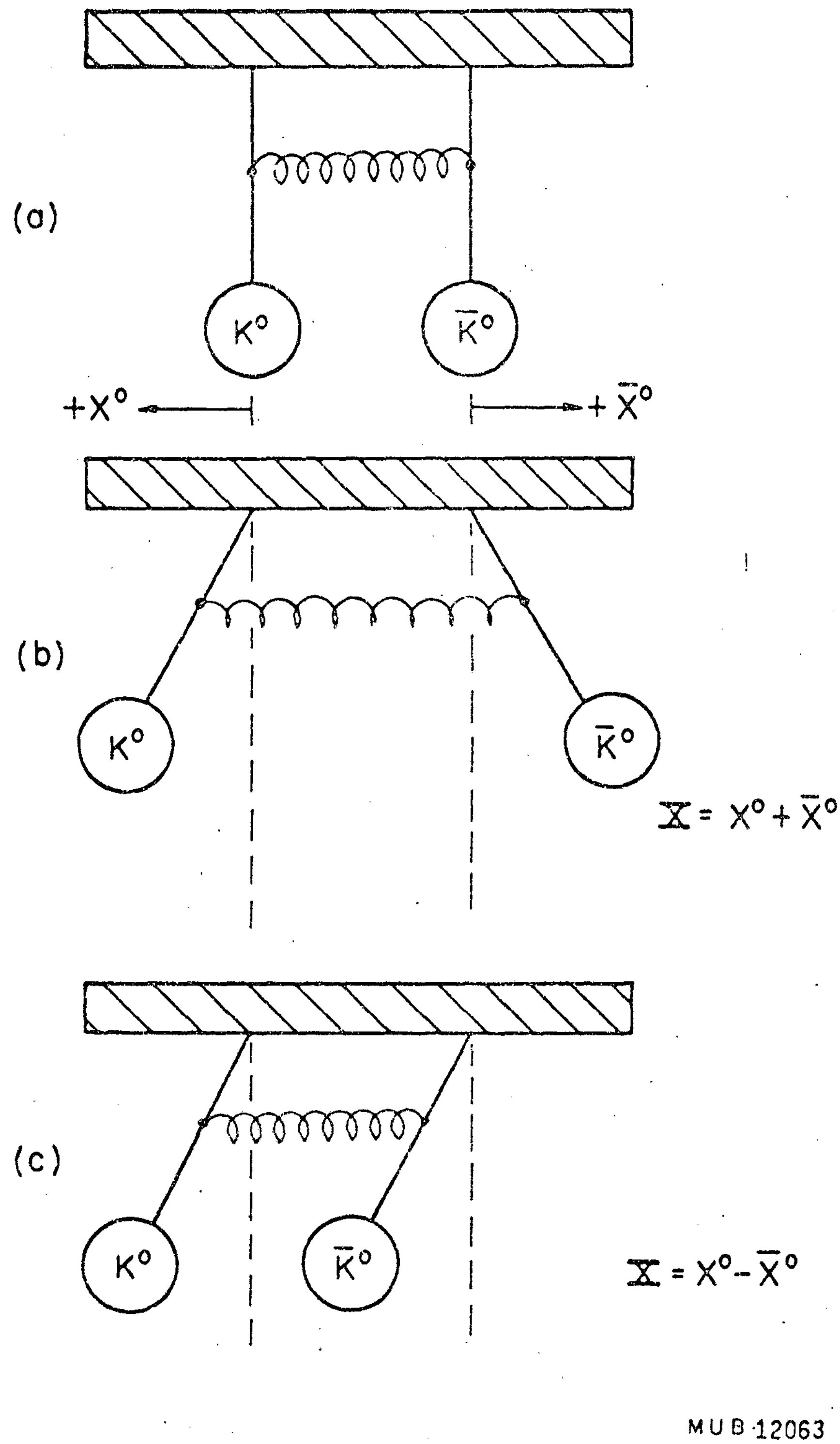

Fig. 1. Coupled pendula: (a) position of equilibrium, (b) normal mode of higher frequency, (c) other normal mode.

$\omega_2 = \sqrt{l/g}$.

The analogy with the quantum mechanical $K^0 - \bar{K}^0$ system is clear. The uncoupled pendula's frequencies represent the masses of the K^0 and $\bar{K}^0$ particles, and the inelastic coupling spring represents the 2π decay mode of the neutral kaon. We can therefore identify the eigenfunction K_1^0 with the short-lived normal mode shown in Fig. 1(b) and the K_2^0 (which "lives" about 600 times as long as the K_1^0) with the mode shown in Fig. 1(c). Notice that since the stiffness coefficient k is always positive, ω_1 is always greater that ω_2 in our pendulum analogy.

To observe the energy transfer from one pendulum to the other, start with the K^0 pendulum displaced from equilibrium, leaving the $\bar{K}^0$ pendulum at rest. The gravitational potential energy of the $\bar{K}^0$ pendulum (proportional to the square of its amplitude) will vary sinusoidally with time, with a period of oscillation governed by a beat frequency $\omega_b = (\omega_1 - \omega_2)/2$. Explicitly, the square of the $\bar{K}^0$ amplitude $(\bar{X}^0)^2 \propto \sin^2[(\omega_1 + \omega_2)t/2]\ \sin^2(\omega_b t)$, and a similar expression holds for $(X^0)^2$. Since the frequency difference between the two normal modes is a function of k, we can insert a stiff (weak) spring in our mechanical model to show a rapid (slow) energy transfer between the K^0 and $\bar{K}^0$ pendula.

The analogy with the quantum mechanical $K^0 - \bar{K}^0$ system is direct. If we initially have a beam of K^0's, at some later time we will have a fraction of $\bar{K}^0$'s in the beam, the amount being governed by the frequency difference (or mass difference) between the K_1^0 and the K_2^0. The fraction of K^0 and $\bar{K}^0$ in the beam varies with time in a manner shown in Fig. 2(a) and 2(b), where we assume $|m_1 - m_2| = 0.57\,\tau_1^{-1}$. Abscissas are in units of τ_1. If the kaons have an average momentum of 500 MeV/c, the maximum buildup of the $\bar{K}^0$ component occurs at a comfortable experimental distance of ≈9 cm from the production point of the K^0. We can therefore easily measure the $K_1^0 - K_2^0$ mass difference by this method of producing K^0's with a momentum near 500 MeV/c (in a medium such as hydrogen) and of looking for the time development of $\bar{K}^0$'s. In accord with the mechanical pendula problem, where the

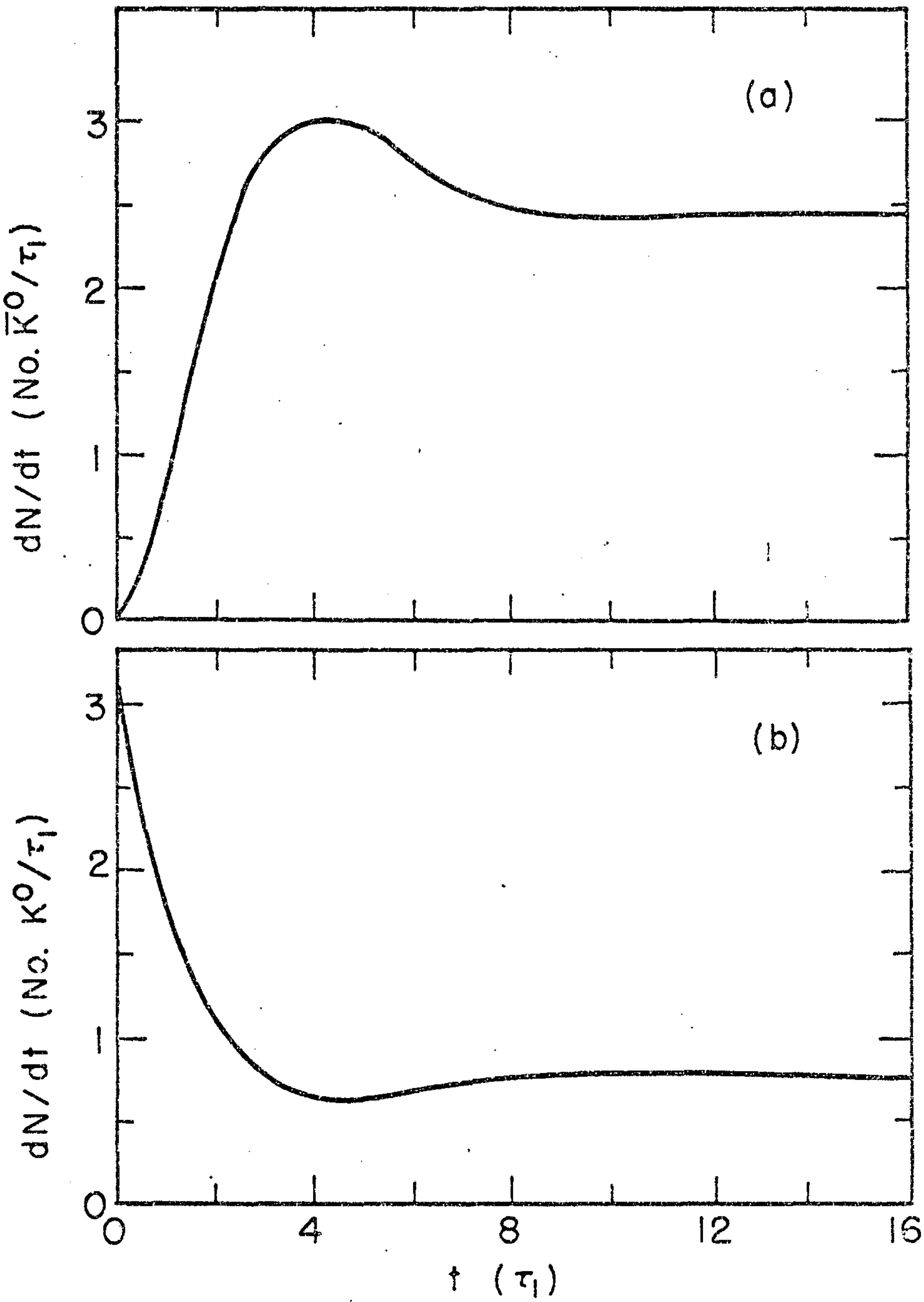

MUB-12068

Fig. 2. Unnormalized counting rate for (a) $\overline{K}^0p$ inelastic interactions and (b) K^0p charge-exchange reactions from an initial K^0 beam for $|m_1-m_2| = 0.57\,\tau_1^{-1}$.

beat frequency of energy transfer enters as $\sin^2(\omega_b t)$, we can measure only the magnitude of the K_1^0-K_2^0 mass difference, using this technique of following the development with time of the square of the amplitude.

To measure the sign of the K_1^0-K_2^0 mass difference requires study of neutral K scattering followed by K_1^0 decay. It is also possible to simulate this phenomenon with our coupled pendula system. To understand the analog, remove, in Eq. (4), $(A+\bar{A})$ as a common factor;[14] we thus have, with $|R| \exp(i\theta) \equiv (A-\bar{A})/(A+\bar{A})$, the K_1^0 amplitude proportional to

$$a_1 = \exp(-im_1 t - \lambda_1 t/2) + |R| \exp[i(\theta - m_2 t) - \lambda_2 t/2]. \qquad (6)$$

If $|R|$ is close to one, Eq. (6) is very similar to Eq. (3a), the only difference being an additional relative phase shift of θ. All information about the sign of the mass difference is contained in the interference term of the absolute square of Eq. (6). This term is $\propto \cos[(m_1-m_2)t+\theta]$, so that θ must be near $\pi/2$ if we hope to determine the sign of m_1-m_2. In fact, as will be discussed in Sec. IV, θ is near $\pi/2$. This fact plus the measured value of $|m_1-m_2|$ enables us to calculate the expected time distribution of elastic scatters followed by K_1^0 decay for either sign of the mass difference. The counting rate for the two cases will show the greatest difference when t equals one- or three-quarters of a beat frequency period T. This rate will show an enhancement at $t = \frac{1}{4}T$ if $m_1 - m_2$ is negative, but if $m_1 - m_2$ is positive, there will be an enhancement at $t = 3/4\ T$.

To demonstrate negative (positive) $m_1 - m_2$ with pendula, one should start with an initially displaced K^0, wait for one-quarter (three-quarter) of the period of time necessary for a complete cycle of energy transfer, and at this point shift the phase of the K^0 90 deg with respect to the $\bar{K}^0$. In practice this maneuver would mean that one should delay the $\bar{K}^0$ pendulum for one-quarter of its uncoupled period. A pure K_1^0 mode would then remain.

III. EXPERIMENTAL PROCEDURE

A. The Beam

During the fall of 1960 and spring of 1961, the Alvarez 72 inch hydrogen bubble chamber was exposed to a π^- beam of 1030 and 1170 MeV/c. The beam-transport system, designed and built by Professor Frank S. Crawford, Jr., has been described previously[15]; we shall therefore mention only briefly some of its characteristics.

A schematic diagram of the beam optics is given in Fig. 3. The most important characteristic of the beam is its excellent momentum resolution (the full width at half maximum of the momentum distribution is ≈ 10 MeV/c.

At 1170 MeV/c there were $\approx 9 \times 10^4$ sets of pictures taken, and $\approx 3 \times 10^5$ triads at 1030 MeV/c. Approximately 17 tracks per picture entered within a chosen fiducial area. The magnetic field strength was 17.91 kG at the bubble chamber for the higher momentum and 15.70 kG for the lower.

B. Scanning

The film was scanned for associated production events involving a visible lambda decay:

$$\pi^- + p \rightarrow \Lambda + K^0, \quad \Lambda \rightarrow p + \pi^- \qquad \text{(4771 events)} \qquad (7a)$$

$$\pi^- + p \rightarrow \Sigma^0 + K^0, \quad \Sigma^0 \rightarrow \Lambda + \gamma, \quad \Lambda \rightarrow p + \pi^- \qquad \text{(1269 events)} \qquad (7b)$$

These events were measured and analyzed in a manner standard to the Alvarez group,[16] with a "Frankenstein" used as measuring projector. When reactions (7) were thoroughly processed, a special scan along the direction of the missing K^0 was performed. Scanners searched along the calculated direction of the missing neutral for interactions or decays that may have been missed in the initial scan. We required no minimum length of the neutral K since the topology for associated production with visible lambda decay, plus a zero-length K^0 interaction or decay, is so striking that such an event would not be missed on the rescan.

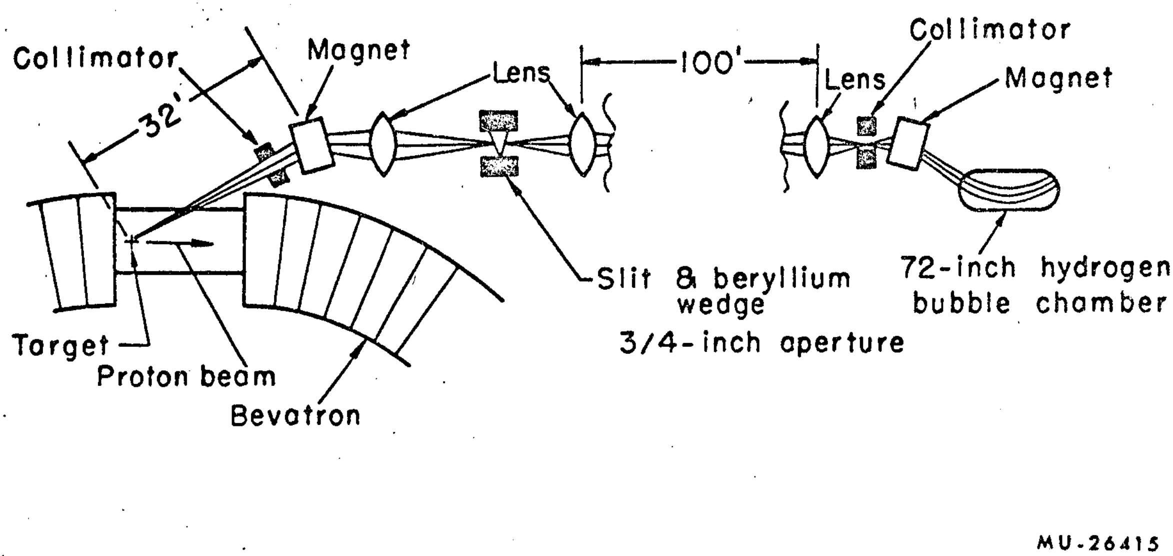

Fig. 3. Schematic diagram of the beam optics.

We consider ΛK^0 and $\Sigma^0 K^0$ production separately.

1. <u>ΛK^0 Production</u>

The missing K^0 direction is known typically to within ± 0.4 deg in dip and azimuth, and the missing K^0 momentum to $\pm 1.5\%$. We scanned along the missing K^0 direction, using a protractor, and provisionally accepted all interaction candidates within ± 5 deg in azimuth of the predicted direction. We believe our scanning efficiency is essentially 100%.

2. <u>$\Sigma^0 K^0$ Production</u>

The missing K^0 direction is poorly known (because of the undetected γ from $\Sigma^0 \rightarrow \Lambda + \gamma$). We rescanned these pictures only for neutral K interactions followed by a $\pi^+\pi^-$ decay. The pictures are clean (about 17 beam π^- per picture), and we believe the second-scan efficiency is 100% for these secondary events. The background is negligible, and there are no spurious or ambiguous events.

We do not use any events where the Λ produced in association with the K^0 in reaction (7) does not decay visibly. If we did, we could guarantee 100% scanning efficiency for K interactions, independent of time t, only by scanning the entire film many times. As it is, no bias is introduced if some associated-production events are not detected, provided we find all K interactions associated with our sample of visible Λ's from reaction (7). Another reason for demanding visible Λ's in reaction (7) is that we thereby completely eliminate the possibility of an ambiguity between two possible production vertices. A third reason is that the information from the Λ decay eliminates some kinematical ambiguities that might otherwise remain.

C. <u>Data Processing</u>

All neutral K interactions of the following types were analyzed:

$$
\begin{aligned}
\overline{K}^0 + p \quad \rightarrow \quad & \Lambda + \pi^+ \\
& \Sigma^0 + \pi^+ \\
& \Sigma^+ + \pi^0 \\
& \Lambda + \pi^+ + \pi^0 \\
& \Sigma^+ + \pi^- + \pi^+ \\
& \Lambda + \pi^+ + \gamma
\end{aligned}
\qquad (8a)
$$

$$\begin{aligned} K^0 + p &\rightarrow K^+ + n \\ K_{neutral} + p &\rightarrow K_{neutral} + p. \end{aligned} \qquad (8c)$$

Measurements and kinematical analysis of these events were done in a manner similar to that used in the analysis of reactions (7). For those events which proved to be especially troublesome, the Alvarez Group QUEST system[17] was used. We use χ^2 cutoffs, at the 0.3% probability level, of 8.6, 11.6, 14.0, and 16.0, for one-, two-, three-, and four-constraint fits, respectively.

Reactions of type (8a) were used to measure $|m_1 - m_2|$ (Ref. 1), and these plus reactions (8b) are to be used in a test of CP, T, and CPT invariance as proposed by Crawford.[18]

Reactions (7) plus (8c), in which the final $K_{neutral}$ is detected by the visible decay $K_1^0 \rightarrow \pi^+\pi^-$ (double-vee events), are used in the analysis for the sign of the $K_1^0 - K_2^0$ mass difference. There is no cutoff

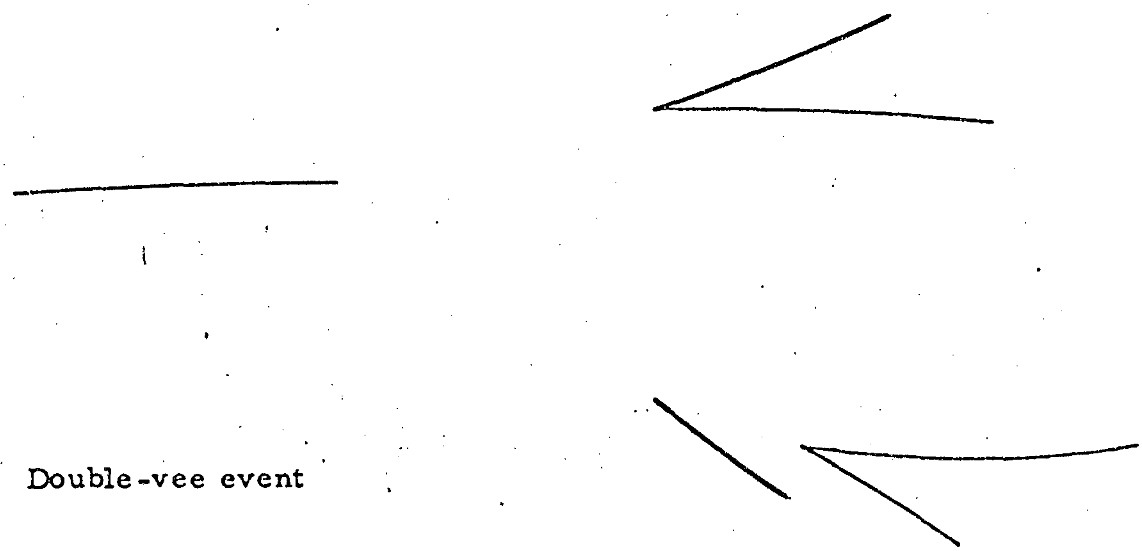

Double-vee event

on the length of the recoil proton. We find 23 double-vee events with initial K^0 momentum $P_K < 601$ MeV/c; these are summarized in Table I. Six similar events with $P_K > 601$ MeV/c are not used because of lack of information on the I = 1, $\bar{K}N$ (S = -1) scattering amplitudes above 600 MeV/c. These events are summarized in Table II. Our demand for a visible Λ decay gives us essentially 100% detection efficiency for finding double-vee events. There are no ambiguous events and no background.

Table I. Summary of 23 double-vee events. Here t and T are the actual and potential proper times for the elastic scatters, in units of 10^{-10} sec, P_K is the K^0 lab momentum in MeV/c, θ is the angle between the incident and outgoing K^0 in the K-p c.m., f and g are the non-spin-flip and spin amplitudes for elastic K^0-p scattering (solution Y), $\bar{f}$ and $\bar{g}$ are the same for elastic $\bar{K}^0$-p scattering (solution KT), and w is $\log_{10}[50\, p_i(t_i)]$ for $m_1 - m_2 = -0.57\ \tau_1^{-1}$, KT + Y.

Event	t	T	P_K (MeV/c)	Cosθ	f	g	$\bar{f}$	$\bar{g}$	w
528328	0.55	11.74	490.5±6.4	.02	-.09+i.10	.14+i.06	-.01+i.49	-.26+i.02	0.387
533615	21.63	28.51	600.7±4.8	-.33	-.20+i.10	.27+i.11	-.09+i.45	-.41-i.01	0.239
557391	42.79	53.17	322.9±5.5	-.65	-.20+i.04	.08+i.00	-.03+i.40	-.07+i.00	-.054
562253	0.41	11.43	413.7±7.0	-.62	-.25+i.06	.13+i.01	-.05+i.44	-.14+i.00	0.737
583074	2.36	4.15	546.6±9.1	-.08	-.11+i.11	.19+i.09	-.03+i.49	-.34+i.02	1.182
591424	1.95	19.68	563.1±5.1	-.91	-.57+i.06	.16+i.03	-.14+i.41	-.17-i.02	0.617
602450	12.33	16.21	539.1±4.8	-.96	-.58+i.06	.10+i.02	-.13+i.42	-.10-i.01	0.380
683243	14.25	20.94	558.7±7.5	-.97	-.62+i.06	.10+i.02	-.14+i.41	-.10-i.01	0.285
691160	0.87	14.08	546.4±8.7	-.95	-.58+i.06	.12+i.02	-.13+i.42	-.12-i.02	0.903
773436	1.27	9.27	299.5±1.1	.03	-.08+i.04	.03+i.00	-.00+i.40	-.07+i.01	0.683
778118	4.27	25.76	260.5±3.2	-.37	-.11+i.03	.45-i.00	-.01+i.36	-.05+i.00	0.370
826368	13.58	15.94	349.4±7.2	-.91	-.29+i.05	.06+i.00	-.05+i.41	-.05-i.00	0.422
828583	30.89	57.71	305.3±1.6	-.17	-.10+i.04	.05+i.00	-.01+i.40	-.08+i.00	-.068
837477	16.46	29.63	408.6±2.4	.39	-.07+i.08	.04+i.03	.03+i.49	-.15+i.02	0.232
1363048	4.33	8.18	195.6±3.4	-.68	-.30-i.06	-.13-i.04	-.01+i.30	-.02-i.00	0.697
1479538	8.34	20.54	597.9±3.1	.91	-.14+i.31	-.01+i.08	.23+i.81	-.14+i.05	0.360
1738296	9.39	46.56	325.0±4.3	-.61	-.19+i.04	.08+i.00	-.03+i.40	-.07+i.00	0.022
1760182	11.06	16.83	454.8±3.0	.73	-.08+i.13	.01+i.04	.08+i.56	-.14+i.03	0.484
1815424	24.42	27.09	392.2±4.1	-.83	-.31+i.06	.10+i.01	-.06+i.42	-.09-i.00	0.215
1867430	3.12	8.65	431.3±5.2	.39	-.06+i.09	.05+i.03	.03+i.50	-.17+i.02	0.902
1882600	0.85	18.48	491.1±8.4	-.14	-.13+i.09	.17+i.06	-.03+i.48	-.26+i.01	0.341
1884143	6.63	32.83	329.5±1.4	-.28	-.13+i.05	.07+i.01	-.02+i.41	-.09+i.00	0.187
1886184	32.01	43.66	274.9±1.4	-.08	-.08+i.03	.03+i.00	-.00+i.38	-.06+i.00	0.061

Table II. Summary of six double-vee events with $P_K > 601$ MeV/c. Labels are as in Table I.

Event	t (10^{-10} sec)	T (10^{-10} sec)	P_K(MeV/c)	Cos θ
1359080	0.12	13.86	754.7±14.2	0.10
1449290	9.36	17.54	793.2± 5.2	0.79
1450126	4.02	12.51	644.6± 3.8	-0.74
1483150	10.65	16.94	698.4± 4.5	-0.81
1484108	0.25	11.01	810.8± 4.1	0.81
1815348	8.20	20.13	648.0± 3.3	-0.95

In those cases where the strange particle produced in reactions (8) does not decay, background "recoils" become a problem. In these instances, the positive track in reactions (8) is sometimes indistinguishable on the scanning table from a proton recoil arising from an n-p scatter due to neutron background. There are about 900 such candidates (i.e., about 15% of the missing K^0's have a random recoil proton lying within ±5 deg). We measure the neutral "track" from the production point to the recoil and reduce the amount of background by rejecting recoils that have a neutral differing by more than five standard deviations from the predicted K^0 direction.[19] The remaining 300 events are fitted (one-constraint) to reactions (8).

We accepted 13 single-vee events corresponding to K^0 production via reaction (7a) and to subsequent interaction via reaction (8c) without a subsequent visible K_1^0 decay. Eleven of these are unambiguous

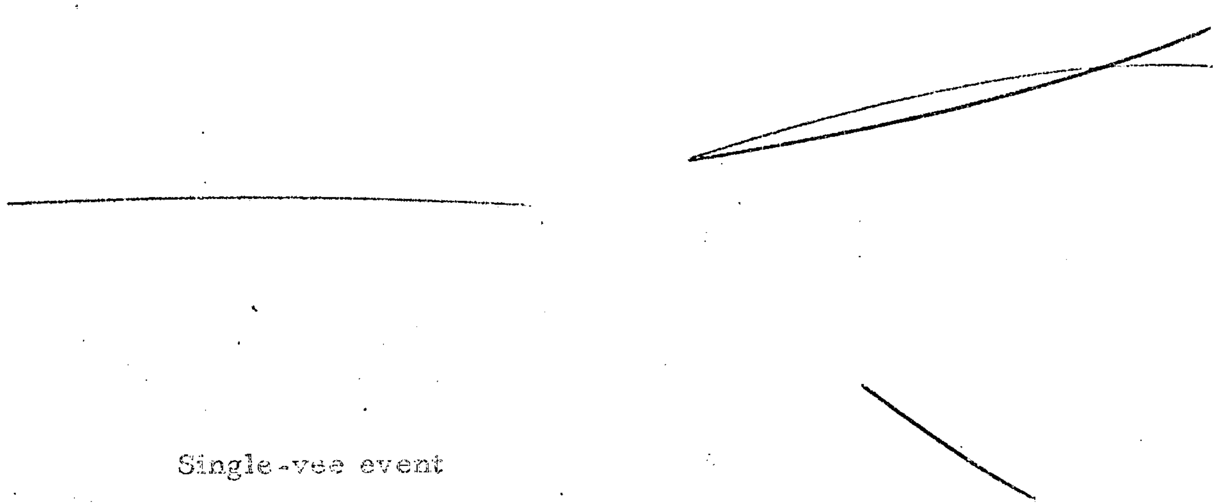

Single-vee event

from their kinematical fits, and the remaining two are resolved by using ionization information. The 13 events are summarized in Table III. For single-vee events we imposed a 1.5-cm minimum length cutoff on the recoil proton, thus reducing our background due to random proton recoils to an estimated 0.2 events. The absence of a visible K_1^0

decay can correspond to either $K_1^0 \rightarrow 2\pi^0$ or to K_2^0 leaving the chamber without decaying. This ambiguity leads to a washing out of information on the sign of $m_1 - m_2$, and we therefore do not use these 13 events in determining $m_1 - m_2$. We do include them in tests (described below) of the predictions made by the various sets of phase shifts.

Table III. Summary of thirteen single-vee events. Here t and T are the actual and potential proper times for the elastic scatters, P_K is the K^0 lab momentum, and θ is the c.m. scattering angle of the outgoing K with respect to the incident K.

Event	t (10^{-10} sec)	T (10^{-10} sec)	P_K (MeV/c)	Cos θ
532155	4.20	20.47	653.3± 6.9	0.36
585259	3.10	9.82	434.9± 4.0	0.74
702127	3.07	11.17	504.0± 5.2	0.07
712366	3.08	15.88	425.6± 5.0	-0.30
781371	10.62	19.84	314.9± 3.4	0.59
845159	3.14	15.94	328.2± 4.3	0.67
859384	0.06	5.52	523.0± 9.9	-0.99
1717243	10.79	20.05	310.1± 3.1	0.57
1722527	11.28	14.90	507.9± 9.6	0.86
1730398	3.47	42.85	528.0±11.1	0.70
1789399	4.30	14.99	539.5± 6.1	0.02
1832576	1.49	15.05	598.0± 8.2	0.33
1845374	10.63	30.44	349.3± 6.3	-0.95

IV. ANALYSIS AND RESULTS

A. Scattering Amplitudes

1. General Remarks

Measuring the sign of the mass difference by the method of Camerini et al. depends on knowing the scattering amplitudes in the KN and in the $\overline{K}N$ channels. Moreover, all information on the sign is lost unless these two amplitudes (A and $\overline{A}$) are mostly relatively imaginary [see Eq. (5)]. We are lucky in this respect. Since the $\overline{K}N$ channel is highly absorptive at the average momentum of our K^0's (450 MeV/c), the elastic scattering amplitude has a large imaginary component. The KN amplitude for elastic scattering, on the other hand, has a large real component. The net result, then, is that the relative phase between A and $\overline{A}$ is close to 90 deg. This statement is imprecise, however, for A is the sum of two noninterfering amplitudes—a non-spin-flip amplitude f and a spin-flip amplitude g. (A similar statement holds for $\overline{f}$, $\overline{g}$, and $\overline{A}$.) Thus there are two independent phases—a relative phase between the non-spin-flip amplitudes f and $\overline{f}$ and one between the spin-flip amplitudes g and $\overline{g}$. Therefore each coefficient of the time-dependent terms in Eq. (5) has two contributions: one from the non-spin-flip amplitudes and the other from the spin-flip amplitudes. [For example, $\mathrm{Im}\, A^*\overline{A} = \mathrm{Im}(f^*\overline{f} + g^*\overline{g})$.] The relative phases of these two noninterfering amplitudes, for several sets of solutions (described below), are shown graphically in Fig. 4, where we plot f, $\overline{f}$, g, and $\overline{g}$, averaged over our 23 double-vee events.

For $\overline{K}^0$-p scattering we have I = 1, so that $f = \overline{f}^1$ (single superscript now refers to isospin state) and $\overline{g} = \overline{g}^1$. For K^0-p scattering we have both I = 0 and I = 1; thus, $f = \frac{1}{2}(f^0+f^1)$ and $g = \frac{1}{2}(g^0 + g^1)$. With $T^I_{L\pm} = \exp(i\,\delta^I_{L\pm})\sin\delta^I_{L\pm}$, we write f^I and g^I (where I = 0 or 1) in the partial-wave expansion

$$\begin{aligned} f^I &= k^{-1}\sum_L \left[(L+1)\,T^I_{L+} + L\,T^I_{L-}\right] P_L(\cos\theta) \\ g^I &= k^{-1}\sum_L \left[T^I_{L+} - T^I_{L-}\right] P_L{}^1(\cos\theta), \end{aligned} \qquad (9)$$

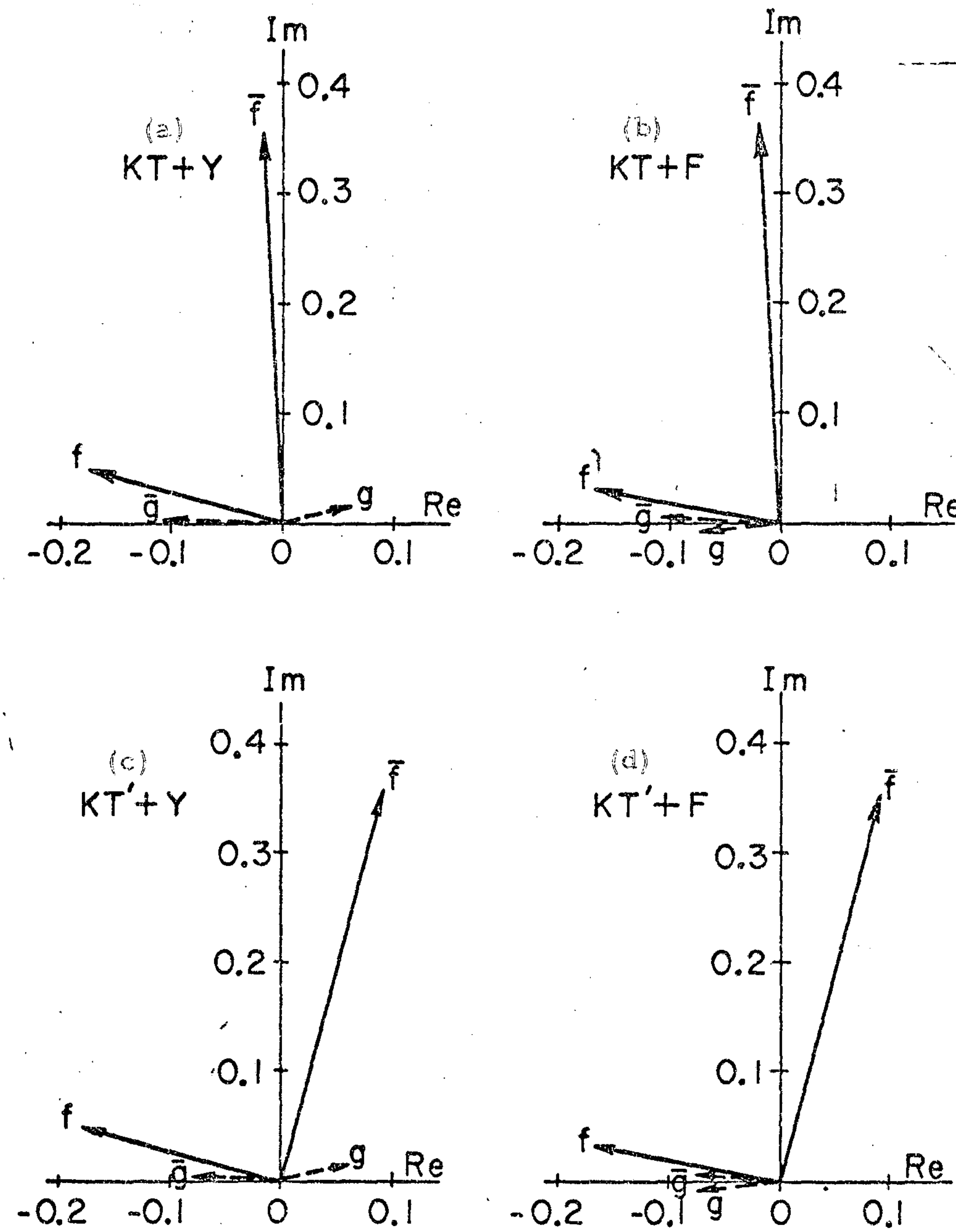

MUB 12065

Fig. 4. Non-spin-flip amplitude $f(\bar{f})$ and spin-flip amplitude $g(\bar{g})$ for K^0p ($\bar{K}^0p$) elastic scattering for solutions (a) KT + Y, (b) KT + F, (c) KT' + Y, and (d) KT' + F.

where the sum is over $L = 0, 1$, and 2, and L+ and L- refer to $J = L + \frac{1}{2}$ and to $L - \frac{1}{2}$. Expressions analogous to Eq. (9) also hold for $\overline{\Gamma}^1$ and $\overline{g}^1$.

The I = 1 KN scattering data[20,21,22] is well satisfied with a constant scattering length up to 640 MeV/c, or with a scattering length plus effective range up to 810 MeV/c, but the I = 0 channel contains a Fermi-Yang-type (F-Y) ambiguity. Slater et al.[23] studied charge-exchange reactions of K^+ in deuterium at momenta of 230, 330, 377, 530, 642, and 812 MeV/c, using the closure approximation; Stenger et al.[24] studied the same film, adding new elastic-scattering data to the charge-exchange data to obtain a different set of I = 0 phase shifts by means of the impulse approximation. Both sets of phase shifts agree within errors, with more p-wave being indicated by the central values of Stenger et al. To get the S = +1 scattering amplitudes, we use the SPD phase shifts of Stenger et al. To obtain a smooth dependence on k [necessary because each of our events has its own K^0 momentum and because now we can easily change S = +1 scattering amplitudes to determine their effect on our likelihood function and on cross sections which are a function of these amplitudes (see Sec. IV A.3)], we fit the phase shifts to a two-parameter expansion $k^{2L+1}\cot\delta_L = (G_L)^{-1} + \frac{1}{2} r_L k^2$. The results are shown in Table IV and in Fig. 5. We make no physical interpretation of the values of these parameters; they give good fits to the phase-shift data.

2. Restrictions on $\overline{K}N$ Amplitudes

Low-energy K^--p experiments by Humphrey and Ross,[25] Kim,[26] and Sakitt et al.[27] have yielded S-wave scattering lengths; Watson, Ferro-Luzzi, and Tripp[28] have analyzed their K^--p data from 250 to 513 MeV/c in terms of the zero-effective-range expansion to obtain scattering lengths for partial waves s, p_1, p_3, and d_3 (subscript equals 2J). We look at the ratio

$$R \equiv \sigma(K_2^0 p \to K_1^0 p)/[\sigma(K_2^0 p \to \Lambda\pi^+) + 2\,\sigma(K_2^0 p \to \Sigma^0\pi^+)]$$

Table IV. Parameters G in units of $(\text{fermis})^{2L+1}$ and r in units of $(\text{fermis})^{1-2L}$ in a fit to the SPD solution of Stenger et al. Superscript is isospin, and subscript is twice total angular momentum J.

		Partial waves					
		S^0	S^1	P_1^0	P_3^0	D_3^0	D_5^0
Yang type	G	0.04	-0.29	0.11	-0.05	0.06	1.0
	r	0.0	0.5	0.0	102.	-65.	-320.5
Fermi type	G	0.04	-0.029	-0.30	0.12	0.001	0.15
	r	0.0	0.5	-61.	4.1	0.0	-64.

as a function of momentum for a given $\bar{K}N$ I = 1, S-wave complex scattering length (we have only one KN scattering solution at low energy since there is no Fermi-Yang ambiguity for S-wave), and compare this dependence with the values of R measured by Kadyk et al.[29] The usefulness of this test in sorting out a multitude of solutions in the $\bar{K}N$ channel was first pointed out by Biswas.[30] Figure 6 shows the experimental values of R from Kadyk et al. and the value from our data at the average K^0 momentum from reactions (7), as well as bands corresponding to central values and standard errors for some of the published sets of scattering lengths. (The smooth curves in Fig. 6 are taken from Kadyk et al.[29]) Humphrey-Ross solution 1 gives results which are consistent with solution I of Watson et al.,[28] so it is not used explicitly. Solution 1 from Sakitt et al.,[27] solution 2 from Humphrey and Ross, and solution II of Kim[26] are not used as possible sets of amplitudes because of their poor predictions for R (see Fig. 6)(last solution also has a poor χ^2 fit to Kim's own data). We used solution 2 from Sakitt et al. and solutions I through IV from Watson et al. in our experiment, even though the upper limit of R, calculated by using these solutions, disagrees with the points of Kadyk et al. by two to three standard deviations at each of the four lowest momenta (P-wave appear to be important above about 350 MeV/c, so we should not take seriously the discrepancy between the experimental value of R at ≈460 MeV/c and the theoretical predictions

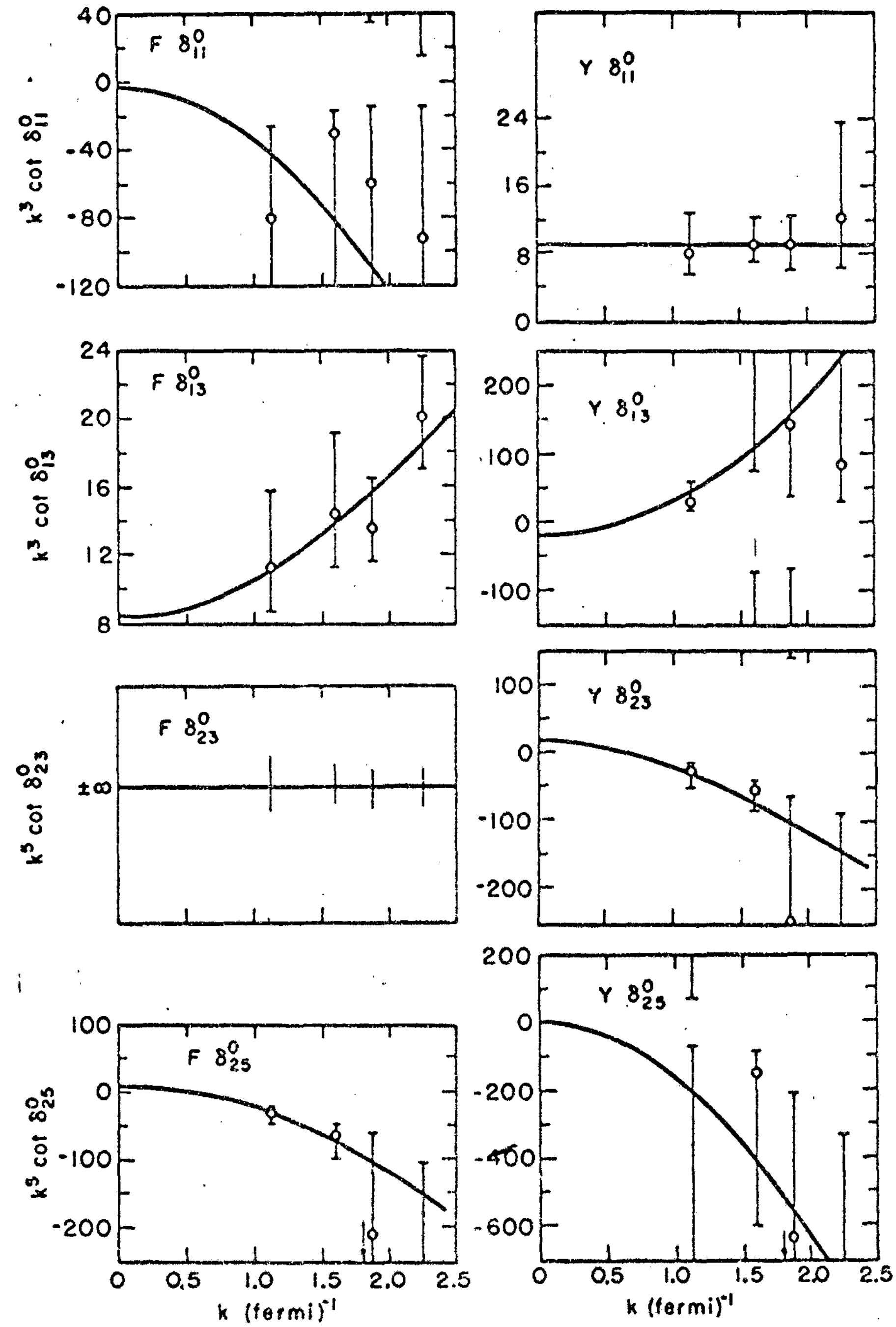

Fig. 5. Fit of two-parameter expansion $k^{2l+1}\cot\delta^I_{l,2j} = (G^I_{l,2j})^{-1} + \frac{1}{2}(r^I_{l,2j})k^2$ to phase shifts of Stenger et al.[24] Y indicates Yang-type solution, and F indicates Fermi type. The arrow indicates our momentum cutoff of 600 MeV/c.

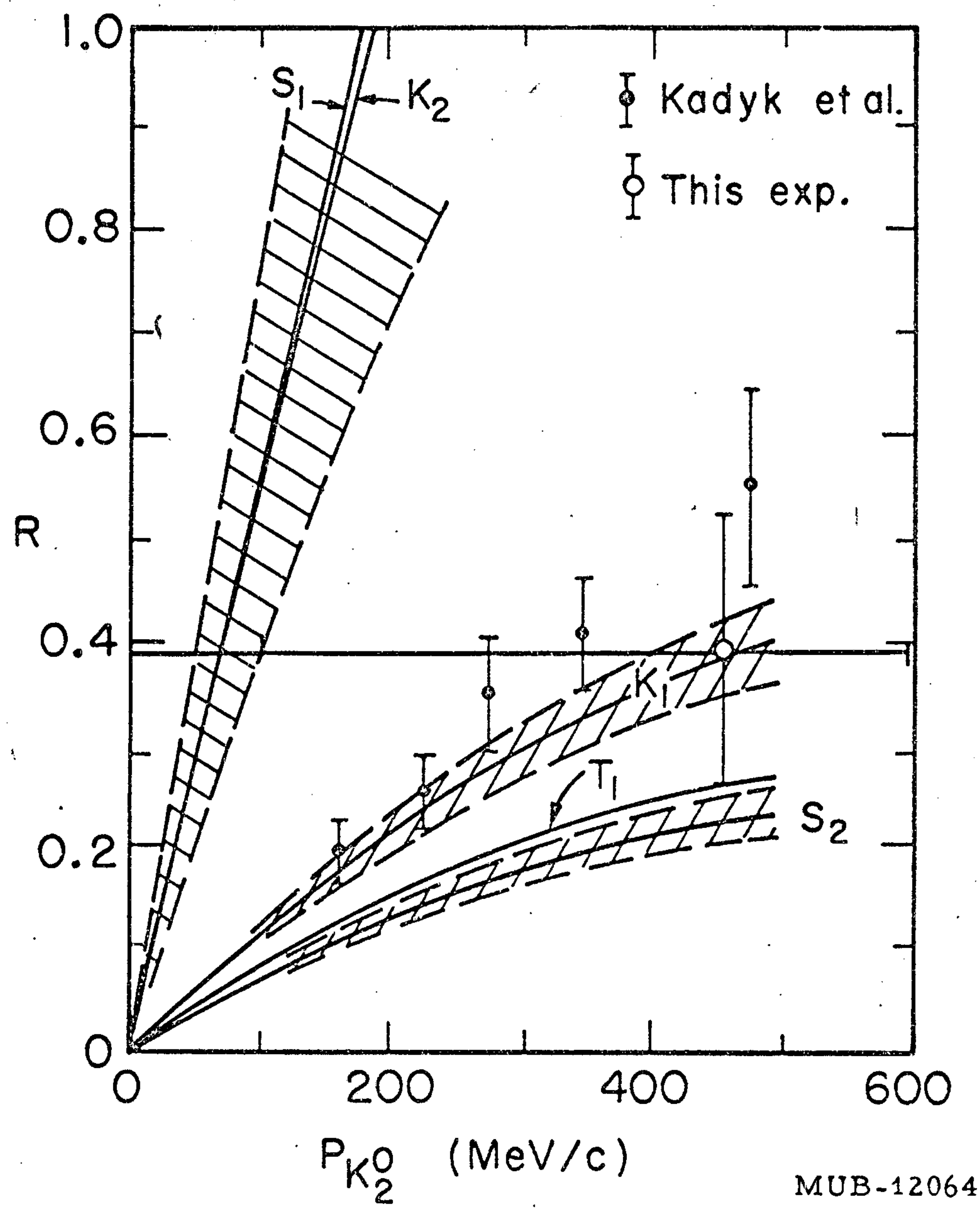

Fig. 6. Experimental values of $R \equiv \sigma(K_2^0 p \to K_1^0 p)/[\sigma(K_2^0 p \to \Lambda\pi^+) + 2\,\sigma(K_2^0 p \to \Sigma^0\pi^+)]$ from Kadyk et al.[29] and values calculated for various sets of scattering amplitudes. T refers to scattering lengths from Watson et al.[28], K refers to Kim[26], and S refers to Sakitt et al.[27]. Subscripts to T, S, and K are solution numbers given in the reference. ——: central values of R; ▨ : regions of uncertainty. (The errors on solution T_1, which overlap those of S_2, are not shown.) Experimental values cover momentum intervals of about 70 MeV/c.

for R, which are based on only S-wave amplitudes). The only solution in good agreement with the measured values for R is solution I of Kim.

We describe here three sets of solutions which we label T(Tripp), KT (Kim-Tripp) and KT'. Solution T is solution I of Watson et al.[28] Solution KT consists of solution I of Kim[26] for $L = 0$, $I = 1$, and solution I of Watson et al. for $L = 1$ and 2, $I = 1$. Our preference for Kim's S-wave scattering length is based partly on the argument given above and partly on our own data (see Sec. IV. A. 3).

3. Comparison of Observed and Predicted Counts

We test a set of solutions by comparing the predicted with the observed number of events produced by our sample of neutral kaons for each of the following six categories: charge-exchange production of K^+; inelastic scattering of $\overline{K}^0$ (hyperon production), and forward- and backward-scattered neutral kaons in double-vee and single-vee events. In using various sets of scattering amplitudes to make predictions for the elastic scattering, we first integrate $I_1 dt$ (I_1 from Eq. (5)) over t from zero to t_{max} ($\equiv T$) for each K^0 from reactions (7) and sum the results. Oscillatory terms from the integrand then average essentially to zero. This fact plus the fact that the potential path is usually large compared to the mean K_1^0 decay path length (the median potential proper time is about 15×10^{-10} sec) lead to predictions that are insensitive to the magnitude and sign of $m_1 - m_2$. Whereas the expected number of events in the first two categories listed above is nearly independent of $|m_1 - m_2|$ [see Eqs. (15) and (16) and Eqs. (17) and (18)], and the predicted number of counts for the last four is insensitive to $m_1 - m_2$, the predictions are, of course, functions of f, g, $\overline{f}$, and $\overline{g}$. We can therefore test the scattering amplitudes before using them to determine $m_1 - m_2$. Since the expected numbers of double-vee and single-vee events are dependent upon interference terms between KN and $\overline{K}N$ amplitudes, we might expect the predicted counts to be sensitive to the various sets of KN and $\overline{K}N$ solutions. This, in fact, is true, and is also the reason for the success of the Biswas ratio R in eliminating some of the many $\overline{K}N$ solutions.

We have 20 double-vee events with momentum less than 600 MeV/c and within the somewhat smaller fiducial volume imposed for the study of absolute rates.

For a K^0 produced at t = 0 with c. m. momentum $\hbar k$, the probability $P_{2v}(x)\,dx$ that a double-vee event will occur at proper time t in lab-distance interval dx and with c. m. scattering angle θ (between the outgoing kaon and the incident direction) in differential solid angle $d\Omega$ is given by

$$P_{2v}(x)\,dx = 0.685\, P_{K_1}(x)\,dx,$$

where 0.685 is the branching ratio $\Gamma(K_1^0 \to \pi^+\pi^-/\Gamma(K_1^0 \to \text{all})$, and where

$$P_{K_1}(x)dx = \frac{1}{8}\xi(t)\, I_1(t,\theta,k)n dx\, d\Omega. \tag{10}$$

Here n is the number of protons per unit volume, and x lies between 0 and x_{max}, with x_{max} determined for each event by the fiducial volume. The factor $\xi(t)$ is an escape correction factor given by $\xi = 1 - \exp(-\lambda_1 T')$, where T' is the escape time of the scattered K_1^0, and is a known function of t for each event. [For most events $\xi(t)$ is approximately 1 except near t = T; in the following we set $\xi(t) = 1$ for simplicity.] Integrating Eq. (10) over Ω and over x from zero to x_{max} for each K^0 from reactions (7) and summing the results, we get the expected number of double-vee events n_{2v}

$$n_{2v} = 0.685\, n_{K_1},$$

where

$$n_{K_1} = (\pi/38.1\times10^3 \text{ mb}) \sum_{i=1}^{N} \eta_i[\tau_1 C_i + T_i D_i + \alpha(\beta E_i + \gamma F_i)] \tag{11}$$

where τ_1 and T are in units of 10^{-10} sec and where $\eta = P_K(\text{MeV/c})/498.0$ is dimensionless. With $\mu = \cos\theta$ and with λ_1, λ_2, and $m_1 - m_2$ in units of 10^{-10} sec^{-1}, we have, in units of $(\text{cm})^2$,

$$C = \int_{-1}^{1}[\,|A+\overline{A}|^2 = |f+\overline{f}|^2 + |g+\overline{g}|^2]\,d\mu$$

$$D = \int_{-1}^{1}[\,|A-A|^2 = |f-\overline{f}|^2 + |g-\overline{g}|^2]\,d\mu$$

$$E = \int_{-1}^{1}[\,|A|^2 - |\overline{A}|^2 = |f|^2 + |g|^2 - |\overline{f}|^2 - |\overline{g}|^2]\,d\mu$$

$$F = \int_{-1}^{1}[\mathrm{Im}(A^*\overline{A} = f^*\overline{f} + g^*\overline{g})]\,d\mu, \qquad (12)$$

and

$$\alpha = 2[\tfrac{1}{4}(\lambda_1 + \lambda_2)^2 + (m_1 - m_2)^2]^{-1}$$

$$\beta = \tfrac{1}{2}(\lambda_1 + \lambda_2)$$

$$\gamma = 2(m_1 - m_2).$$

We plot path length of neutral kaons available for reaction (8c) where a K_1^0 subsequently decays in Fig. 7.

We have a total of 13 unambiguous single-vee events with a contribution of 1.2 counts from six ambiguous events.

For a K^0 produced at $t = 0$ with c. m. momentun $\hbar k$, the probability $P_{1v}(x)\,dx$ that a single-vee event will occur at proper time t in lab-distance interval dx and with c. m. scattering angle θ in differential solid angle $d\Omega$ is given by

$$P_{1v}(x)dx = [0.315 + 1 - \xi(t)]\ P_{K_1}(x)dx + P_{K_2}(x)dx,$$

where 0.315 is the branching ratio $\Gamma(K_1^0 \to \pi^0\pi^0)/\Gamma(K_1^0 \to \text{all})$, where

$$P_{K_2}(x)\ dx = \frac{1}{8}\,\xi(t)\ I_2(t,\theta,k)\,n\,dx\ d\Omega,$$

and where

$$I_2 = |A-\overline{A}|^2 \exp(-\lambda_1 t) + |A+\overline{A}|^2 \exp(-\lambda_2 t) + 2\exp(-\tfrac{1}{2})(\lambda_1 + \lambda_2)t$$
$$\times [(|A|^2 - |\overline{A}|^2)\cos(m_1 - m_2)t - 2\,\mathrm{Im}A^*\overline{A}\sin(m_1 - m_2)t]. \qquad (13)$$

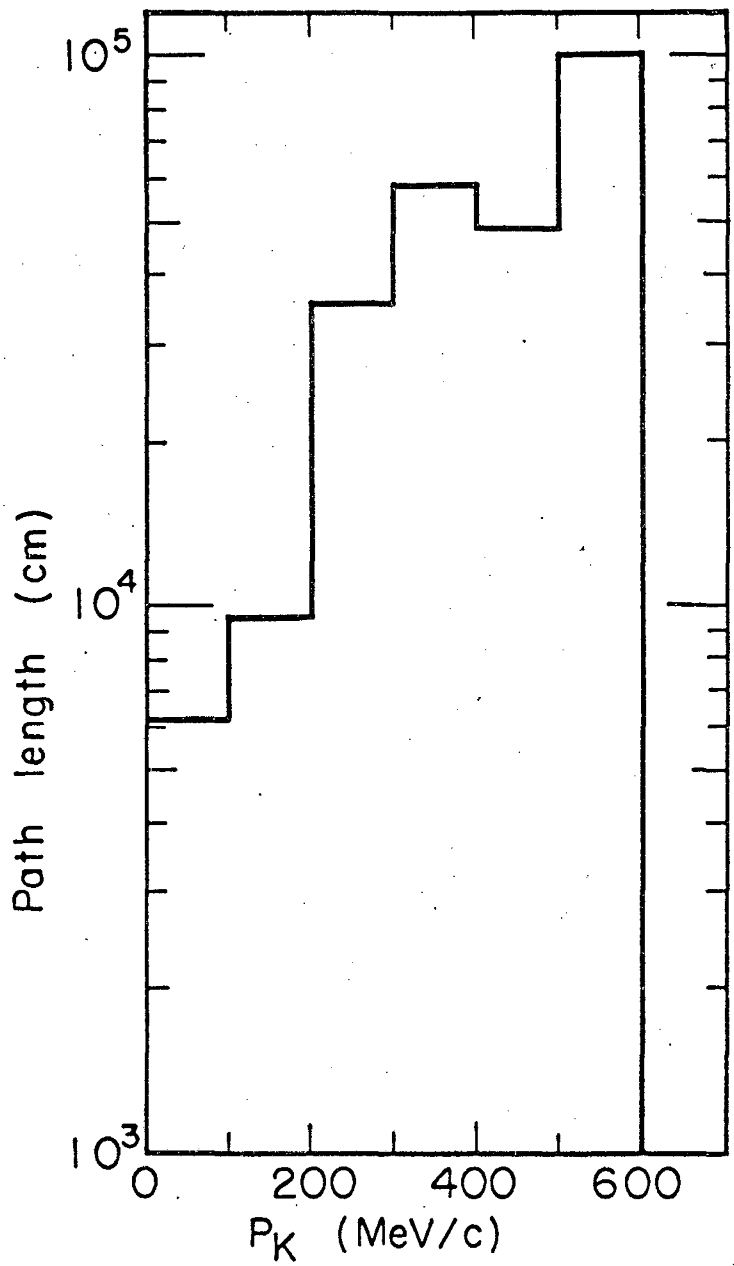

MUB-12067

Fig. 7. Path length available for the reaction $K_{neutral}p \to K_1^0 p$ for six momentum intervals from reactions(7).

Integrating as before and summing only over K^0's from reaction (7a) (indicated by a superscript Λ), we get the expected number of single-vee events n_{1v} [again setting $\xi(t) \equiv 1$ for simplicity]:

$$n_{1v} = 0.315 n^{\Lambda}_{K_1} + n^{\Lambda}_{K_2},$$

where

$$n^{\Lambda}_{K_2} = (\pi/38.1\times10^3 \text{ mb})^{-1} \sum_{i=1}^{N^{\Lambda}} \eta_i[\tau_1 D_i + T_i C_i + a(\beta E_i - \gamma F_i)]. \tag{14}$$

Events of type (8a) and (8b) having no interference between the different strangeness channels, are relatively insensitive to the various scattering solutions. We have nine unambiguous $S = +1$ charge-exchange events from reaction (8a) and 1.3 event prorated from six ambiguous events in the momentum interval considered.

The expected number of charge-exchange events n_{K^+n} is calculated from the expression:

$$n_{K^+n} = (28.6\times10^3 \text{ mb cm})^{-1} \sum_{i=1}^{N^{\Lambda}} \sigma_i L_i . \tag{15}$$

Here L_i is the potential path over which the ith associated production kaon is a K^0, and σ_i is the charge-exchange cross section at the momentum of the ith kaon from reaction (7a). From Eq. (3a) we have

$$L = \ell(4T)^{-1} \int_0^T [\exp(-\lambda_1 t) + \exp(-\lambda_2 t) + 2\exp(-\tfrac{1}{2}(\lambda_1+\lambda_2 t) \cos(m_1 - m_2)t]\, dt, \tag{16}$$

where T is the potential proper time and ℓ is the potential path of the neutral kaon from reaction (7a). With the assumption of charge independence, the cross section σ is given by

$$\sigma = 2\pi \int_{-1}^{+1} (|\tfrac{1}{2}(f^0 - f^1)|^2 + |\tfrac{1}{2}(g^0 - g^1)|^2) d\mu.$$

Including corrections for ambiguous events, underconstrained three-body interactions, and scan-table cutoffs, we have a total of 7.7 events in addition to the 41 observed unambiguous hyperon interactions with $P_K < 600$ MeV/c.

The expected number of inelastic $\overline{K}^0$ interactions n_Y is given by

$$n_Y = (28.6\times10^3 \text{mb cm})^{-1} \left(\sum_{i=1}^{N^{\Lambda}} \overline{\sigma}_i \overline{L}_i + 0.663 \sum_{i=1}^{N^{\Sigma}} \overline{\sigma}_i \overline{L}_i\right) \tag{17}$$

where 0.663 is the branching ratio $\Gamma(\Lambda\to p\pi^-)/\Gamma(\Lambda\to \text{all})$, and where the first summation is over reaction (7a) and the second is over (7b). (See Sec. III. B.2.) Here $\overline{L}$, in accord with Eq. (3b), is given by

$$\overline{L} = \ell(4T)^{-1}\int_0^T \{\exp(-\lambda_1 t) + \exp(-\lambda_2 t) - [2\exp(-\tfrac{1}{2})(\lambda_1+\lambda_2)t][\cos(m_1-m_2)t]\}dt. \tag{18}$$

The inelastic hyperon cross section $\overline{\sigma}$ is calculated from conservation of probability:

$$\overline{\sigma}_{\text{inelastic}} \equiv \overline{\sigma} = \sigma_{\text{total}} - \sigma_{\text{elastic}}.$$

We use the optical theorem to calculate the total cross section $\sigma_{\text{total}} = 4\pi k^{-1}\text{Im}\, \overline{f}^1(\theta=0)$; the elastic cross section is given by $\sigma_{\text{elastic}} = 2\pi \int_{-1}^{+1} (|\overline{f}^1|^2 + |\overline{g}^1|^2)d\mu$.

We use 12 different sets of KN and $\overline{K}$N scattering amplitudes as starting points in a search for solutions which give better predictions for our six mass-independent data than do the original solutions. The predictions of some of the starting solutions as well as our data are given in Table V. None of the starting solutions fit our data well. It is evident that the front-back asymmetries in the double-vee and single-vee events demand a sizable interference between even and odd partial waves. If we collect coefficients of powers of $\cos\theta$, the scattering amplitude $F \equiv \overline{A} - A$, including partial waves through d_5, may be written as

$$kF(\mu) = (S + P\mu + D\mu^2)_{\text{non-spin-flip}} + \sin\theta(P' + D'\mu)_{\text{spin-flip}}, \tag{19}$$

where, in terms of the partial-wave amplitudes,

$$
\begin{aligned}
S &= s - d_3 - 1.5d_5 \\
P &= p_1 + 2p_3 \\
D &= 3d_3 + 4.5d_5 \\
P' &= p_1 - p_3 \\
D' &= 3(d_3 - d_5).
\end{aligned}
$$

Each of the partial-wave amplitudes is the difference between the $\overline{K}N$ and the KN partial-wave amplitudes (i.e., $s = s_{\overline{K}N} - s_{KN}$), corresponding to the dominant term (T_iD_i) in the formula for predicted number of double-vee events [Eq. (11)]. As can be seen from Fig. 8a and 8b, which shows $kF(\mu)$ at 408 MeV/c for solutions KT + F and KT + Y, only the spin-flip amplitude helps to explain the front-back asymmetry. One way to get a larger asymmetry is to increase P. Bearing in mind that the tail of the $Y^*_1(1385)$ may contribute to the $\overline{K}N$ $p_{3/2}$ amplitude,[31] we modify solution KT by changing the real part of the $p_{3/2}$ scattering length from +0.0409 to -0.0409, and by changing the $p_{1/2}$ scattering length from -0.042 + i0.0092 to -0.1 - i0.015. We label this new solution KT'. We now find good fits to our data (χ^2 = 7.0 and 10.4 for KT' + Y and KT' for F respectively). This fact is reflected in Fig. 8c and 8d where there is more interference between S and P than in Fig. 8a and 8b.

In Fig. 9 we plot S, P, D, P', and D' for various solutions; this time the partial-wave amplitude s, p_1, etc. are the sum of the partial-wave amplitudes from the KN and the $\overline{K}N$ channels. This sum corresponds to the important ~~term~~ in the expression for the total number of K_2^0 counts [term T_iC_i in Eq. (14)]. Figure 9a shows S, P, D, P', and D' for KT + Y. It is clear that this solution will give more counts in the back hemisphere than in the front, since P and D have a relative phase of ≈ 180 deg and have lengths greater than D' and P', which are in phase. Solution KT' + Y, however, not only improves the front-back asymmetry in the double-vee events (counts front/counts back = 5/15) as we have seen above, but also improves the front-back asymmetry evident in the single-vee events where front/back = 10/3. Both of these improvements come about because P gets a larger

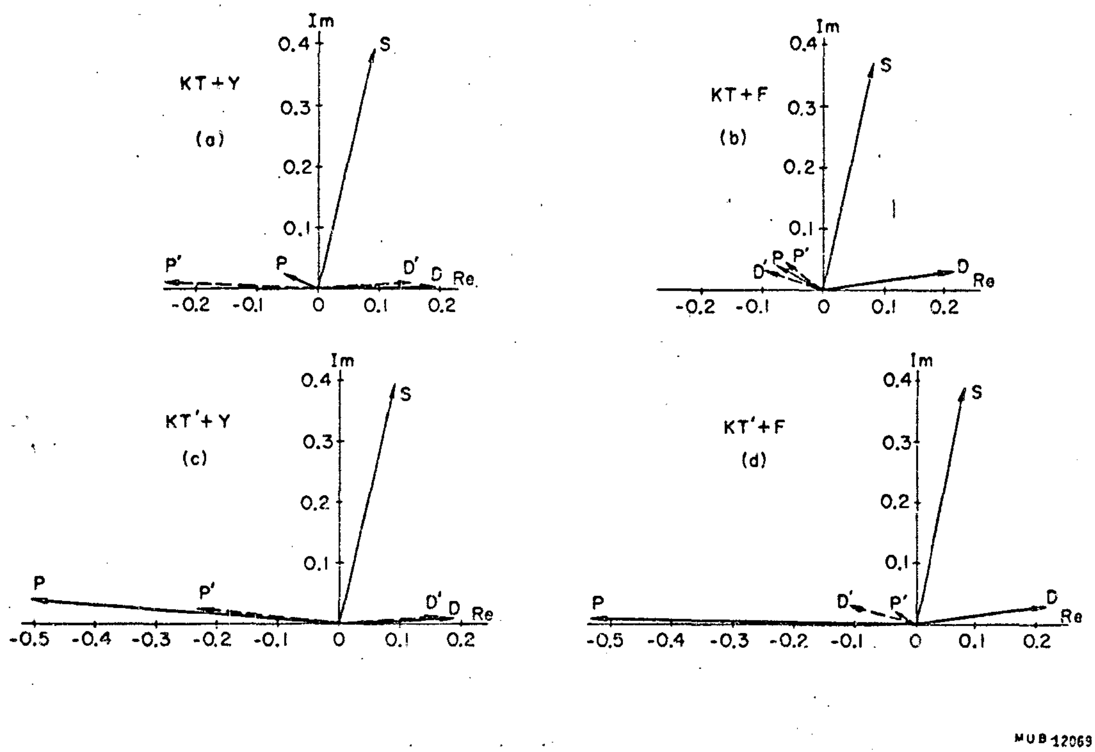

Fig. 8. Coefficients, S, P, D, P', and D' of Eq. (19) at 410 MeV/c for solutions (a) KT+Y, (b) KT+F, (c) KT'+Y, and (d) KT'+F. Each partial-wave amplitude is the difference between those in the KN and $\overline{K}N$ channels.

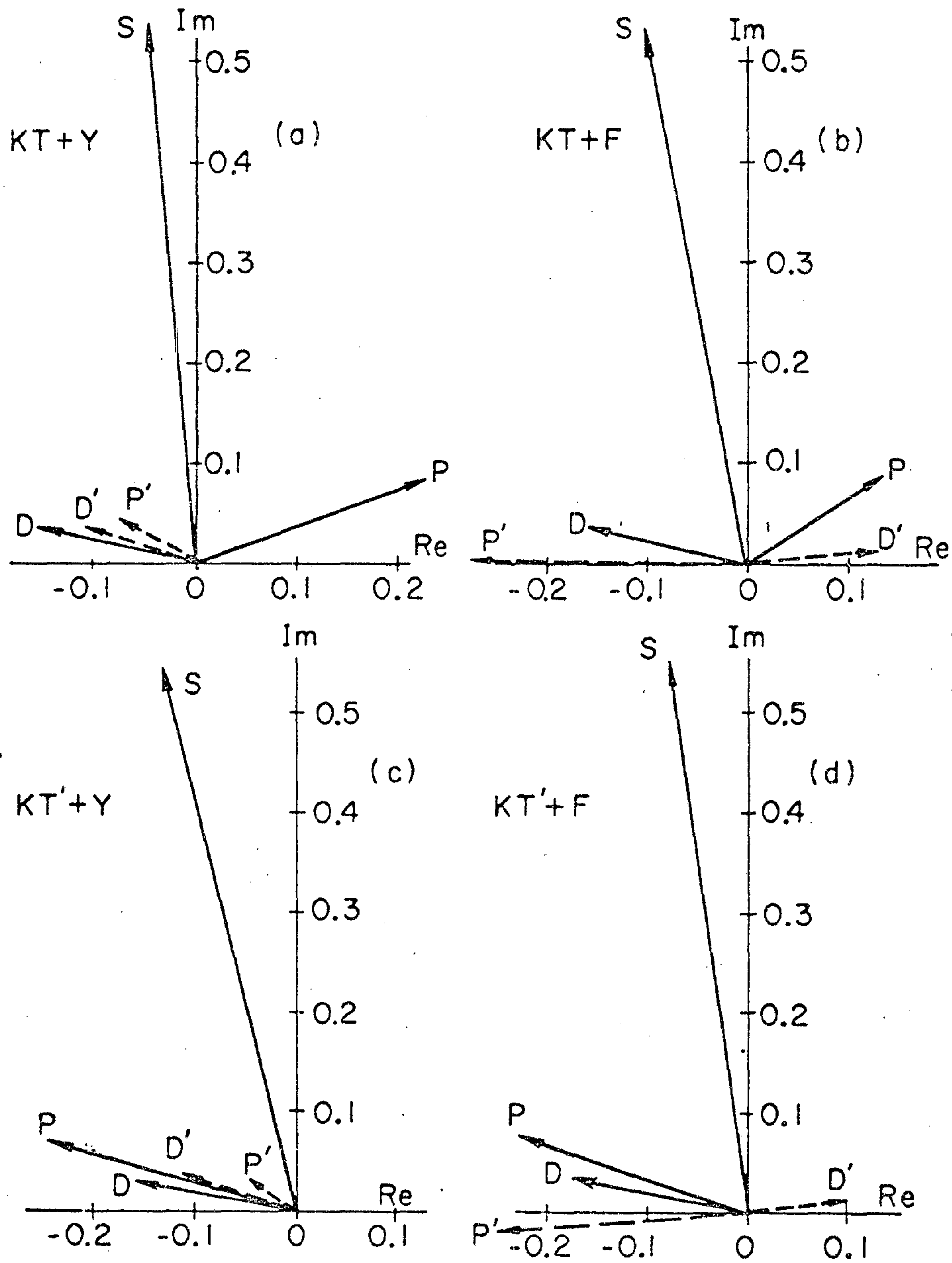

Fig. 9. Coefficients S, P, D, P', and D' of Eq. (19) at 410 MeV/c for solutions (a) KT + Y, (b) KT + F, (c) KT'+ Y, and (d) KT' + F. Each partial-wave amplitude is the sum of those in the KN and $\bar{K}N$ channels.

negative real part due to the changes in the $p_{1/2}$ and the $p_{3/2}$ scattering lengths.

As is evident from Table V, the largest disagreement between the data and the expected number of counts for our best solutions, KT' + F and KT' + Y, is the category of single-vee events in which the neutral kaon scatters backward in the K-p c.m. This category (vi) corresponds to protons of large momentum in the lab system. Single-vee events with long proton tracks should be free from all scanning biases. Since the scanning efficiency for single-vee events is essentially 100%, we conclude that the discrepancy is due either to a statistical fluctuation in this one category or to the use of incorrect scattering amplitudes.

The effect of the various solutions on the $\overline{K}N$ and KN channels is shown in columns eight and nine of Table V. Here the number of pieces of experimental information used are 99 and 18, respectively. The $\overline{K}N$ data used, taken from Watson et al.,[28] are the differential cross sections for K^--p elastic and charge-exchange scattering at momenta of 293, 350, 390, 434, and 513 MeV/c, and the total cross section for K^--p at the same momenta. In the KN channel, we use (from Refs. 20 and 24) the total K^+-p cross section and differential K^+-n charge exchange and non-charge-exchange cross sections at 355 and 520 MeV/c. When we compare solution KT' with the data of Watson et al. (KT' replaces T), we find that the major effect is to increase their χ^2 for $d\sigma/d\Omega$ for K^--p elastic scattering at 390 MeV/c from 35 to 53 ($\langle\chi^2\rangle = 18$), and for charge-exchange scattering from 14 to 25 ($\langle\chi^2\rangle = 9$).

B. Time Distribution, Likelihood Function, and Monte Carlo Results

We find that it makes very little difference to our subsequent time-dependence analysis (to find $m_1 - m_2$) whether we use solutions T, KT, or KT'. [For example, the difference between KT and KT' is largely in the spin-flip amplitude, which is mostly real relative to the KN spin-flip amplitude (see Fig. 4).] We proceed as follows. For a given event i we form a normalized probability distribution function

Table V. Observed and predicted[a] counts for our six categories of events plus the χ^2's for this experiment ($\langle\chi^2\rangle$ is 6), for the $\bar{K}N$ system[b] ($\langle\chi^2\rangle$ is about 95), and for the KN system[c] ($\langle\chi^2\rangle$ is about 13).

	Category[d]								
	i	ii	iii	iv	v	vi	$(\chi^2)_{\text{this exp}}$	$(\chi^2)_{\bar{K}N}$	$(\chi^2)_{KN}$
Observed[e]	9+1.3	41+6.2	5	15	10+0.5	3+0.5	---	---	---
T + Y	9.4	45.6	4.3	5.7	8.1	9.6	20.0	143.3	13.9
T + F	9.4	45.6	3.4	3.4	8.7	11.9	46.7		15.4
KT+Y	9.4	50.8	6.2	7.3	10.8	12.5	15.0	142.6	
KT+ F	9.4	50.8	5.3	5.0	11.4	14.8	28.8		
KT'+ Y	9.4	43.4	6.9	12.5	13.2	11.8	7.0	163.0	
KT'+ F	9.4	43.4	6.2	10.6	13.4	13.5	10.4		

a. Y and F refer to the Yang- and Fermi-type phase shifts in the SPD solution of Ref. 24, T refers to solution I of Ref. 28, and K refers to solution 1 of Ref. 26.

b. Data taken from Ref. 28.

c. Data taken from Refs. 20 and 24.

d. The categories are (i) $K^0p \rightarrow K^+n$, (ii) $\bar{K}^0p \rightarrow$ hyperon, (iii) double-vee events with K scattered forwards (in c.m.), (iv) double-vee events with K scattered backwards, (v) single-vee events with K scattered forwards, and (vi) single-vee events with K scattered backwards.

e. Nonintegers are prorated contributions from six ambiguous events plus corrections to the data.

$p_i(t) = I_i(t)\xi_i(t)/\int I_i(t)\,\xi_i(t)dt$, where the integral is from $T = 0$ to T_i and where $I_i(t) = I(t, \theta_i, k_i)$ from Eqs. (5), (9), and (12), with a given set of scattering amplitudes and with a choice for $m_1 - m_2$. To compare graphically the predicted and observed time distributions, we sum $p_i(t)$ over the 23 double-vee events and plot the result in Fig. 10 for the four cases corresponding to KT + F and to KT + Y, each with $m_1 - m_2 = +0.57$ and -0.57 (in units of τ_1^{-1}, assuming $\tau_1 = 0.88\times10^{-10}$ sec). The observed time distribution is enhanced in the first 2×10^{-10} sec and favors negative $m_1 - m_2$.

We also form a normalized probability-distribution function $q_i(t) = \{[1-.685\,\xi_i(t)]\,I_{1_i}(t) + I_{2_i}(t)\}/\int[0.315\,I_{1_i}(t) + I_{2_i}(t)]\,\xi_i(t)dt$ where $I_{2_i}(t) = I_2(t, \theta_i, k_i)$ from Eqs. (9), (12), and (13), with a given set of scattering amplitudes and with a choice for $m_1 - m_2$. We sum $q_i(t)$ over the 13 single-vee events and plot the result in Fig. 11 for the case KT + Y and $m_1 - m_2 = \pm 0.57\,\tau_1^{-1}$. (The other sets of amplitudes give similar results.) The two curves are not well separated, and moreover, we have only one event in the sensitive region $0.5<t<2.5\times10^{-10}$ sec. It is clear that we lose nothing by not including these events in our analysis for the sign of the mass difference.

Several qualitative results can be drawn from the time distribution of the 23 double-vee events in Fig. 10. One is that the data does not fit the expected time distribution (smooth curves) very well—there are "too many" counts at short time. (We discuss below the statistical significance of this observation.) If we recall the discussion at the end of Sec. II, we note that a relative abundance of counts in an interval near 3×10^{-10} sec favors $m_1 < m_2$. From Sec. II we also learned that the rate of energy transfer from one mode to another was dependent upon the beat frequency of the coupled pendula, or, in the language of neutral kaons, upon the mass difference between the K_1^0 and the K_2^0. The fact that there is a large group of counts at a time less than one-quarter of the beat frequency period ($\approx 2.4\times10^{-10}$ sec) means that our data "prefers" K_2^0 heavier than K_1^0 and $|m_1 - m_2|$ larger than that assumed in the smooth curves in Fig. 10. Another result that can be

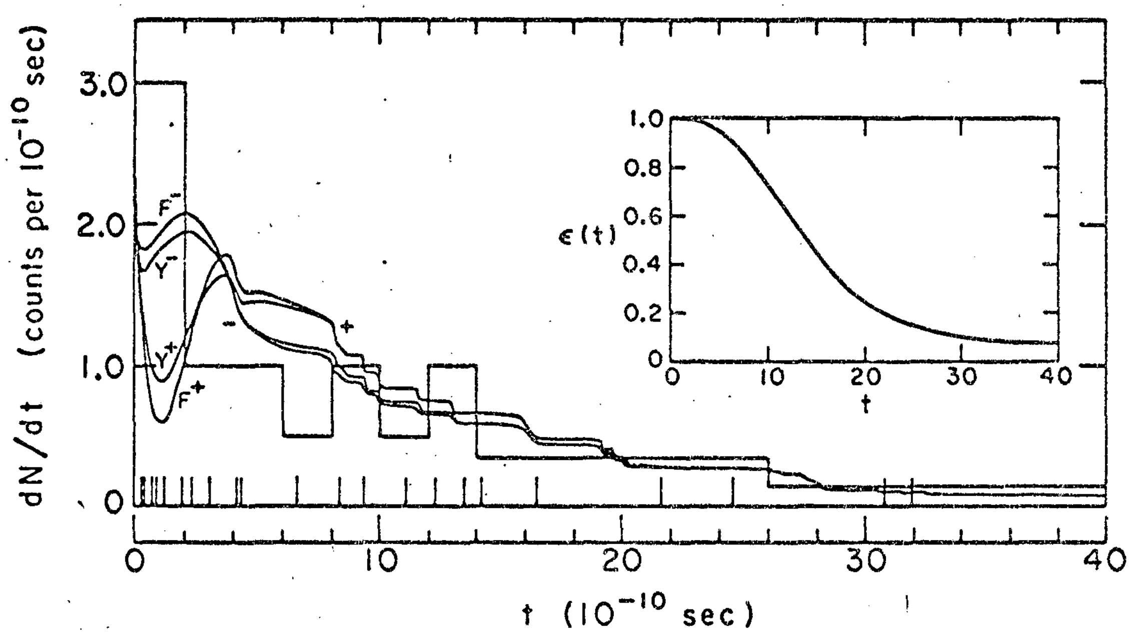

Fig. 10. Time distribution of 23 double-vee events. (One event with $t > 40 \times 10^{-10}$ sec is not shown.) Labels F and Y on the curves refer to phase-shift solutions KT + F and KT + Y, with superscripts + and - referring to $m_1 - m_2 = +0.57$ and -0.57. The curves were constructed by summing $p_i(t)$ over the 23 events; therefore a discontinuity occurs at each time $t = T_i$ (potential proper time for ith event). The individual events are shown as vertical bars. The histogram gives counts per 10^{-10} sec in the indicated interval. The detection efficiency $\epsilon(t)$ is the fraction of the 6040 K^0 mesons having potential time $T > t$.

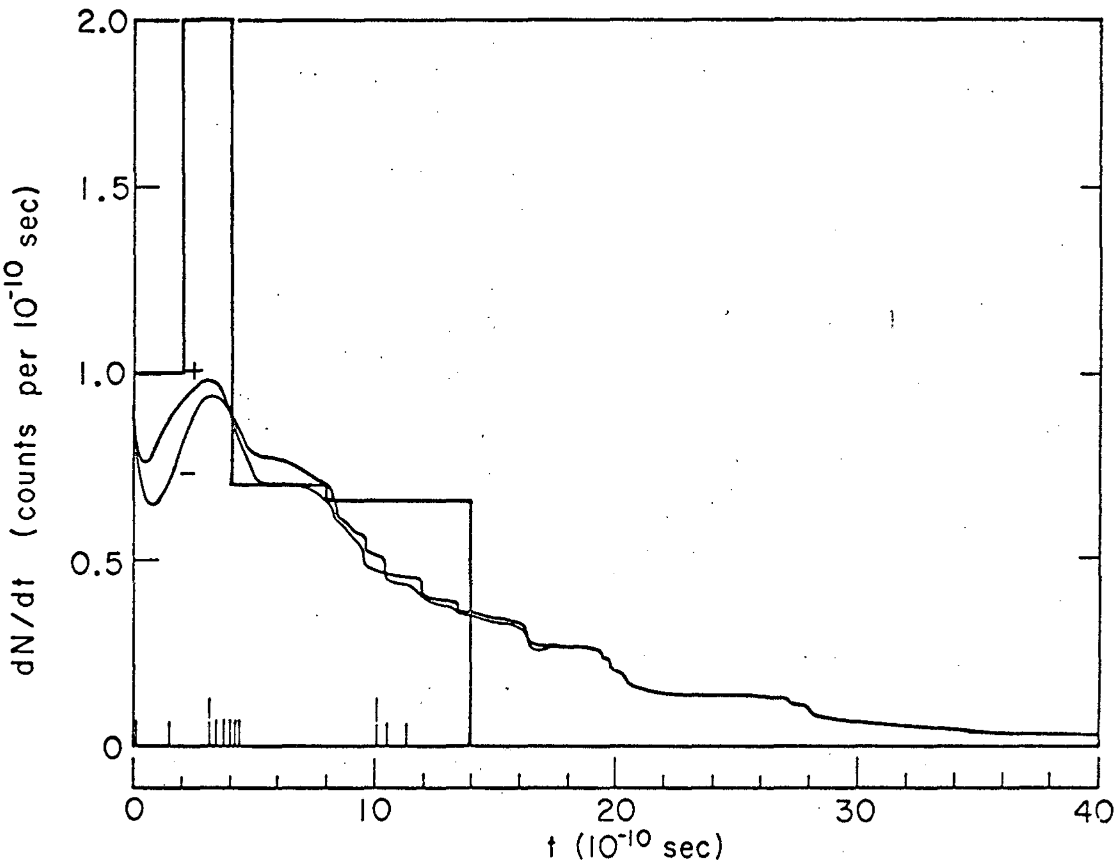

Fig. 11. Time distribution of 13 single-vee events. The curves correspond to solution KT + Y, $m_1 - m_2 = \pm 0.57\ \tau_1^{-1}$. Individual events are shown as vertical bars. The histogram gives counts per 10^{-10} sec in the indicated interval.

drawn from Fig. 10 is that, on the basis of the time distribution alone, one cannot differentiate between the two sets of scattering amplitudes KT + Y and KT + F.

To use all of the information in the 23 double-vee events, we form a likelihood function $\mathcal{L}(m_1 - m_2)$ by setting $t = t_i$ in $p_i(t)$ and taking the product over the 23 events, $\mathcal{L} = \prod_i 50\, p_i(t_i)$, for a given set of scattering amplitudes. (The factor 50 is a convenient normalization factor.) The results for solutions KT + F and KT + Y are shown in Fig. 12. (Those using KT' are very similar and are not shown.) The fact that $\mathcal{L}(m_1 - m_2)$ does not have its maximum value near the known magnitude $|m_1 - m_2| \approx 0.57$ has given us concern. We find that varying the phase shifts or scattering lengths within reasonable limits has little effect on the shape of $\mathcal{L}(m_1 - m_2)$. Monte Carlo studies have convinced us that, with only 23 events, we have suffered a reasonable statistical fluctuation; for a "true" value of $m_1 - m_2 = -0.57$ we find only a 30% probability that $\mathcal{L}$ will have a maximum somewhere between $m_1 - m_2 = -1$ and $+1$.

We also use the Monte Carlo (MC) method to estimate the "goodness of fit" (see Fig. 10) in a manner entirely analogous to the χ^2 tests that one can use with a larger sample of events. We simulate many "experiments" of 23 events each. In each MC experiment, each of the 23 events has the same values of momentum k_i, scattering angle θ_i, and potential time T_i as one of the 23 events of the real experiment, but the time of the scatter, t_i, is chosen according to the <u>a priori</u> probability function $p_i(t)$ for that real event.[32] For scattering amplitude set KT + Y (KT + F), the real experiment gives $\log_{10} \mathcal{L}(-0.57) = 9.58\ (10.00)$. We generate 1000 MC experiments using these sets of amplitudes, according to $m_1 - m_2 = \pm 0.57$. The result of these experiments is that if the hypothesis $m_1 - m_2 = -0.57$ is correct, then the most probable value for $\log_{10} \mathcal{L}(-0.57)$ is 9.85 (9.80), with two-thirds of the MC experiments giving values between 9.20 and 10.55 (9.25 and 10.50). Thus the fit of the data to the hypothesis $m_1 - m_2 = -0.57$ is good. Similarly, the real experiment gives $\log_{10} \mathcal{L}(+0.57) = 8.72\ (8.02)$. The MC result is that if the hypothesis $m_1 - m_2 = +0.57$

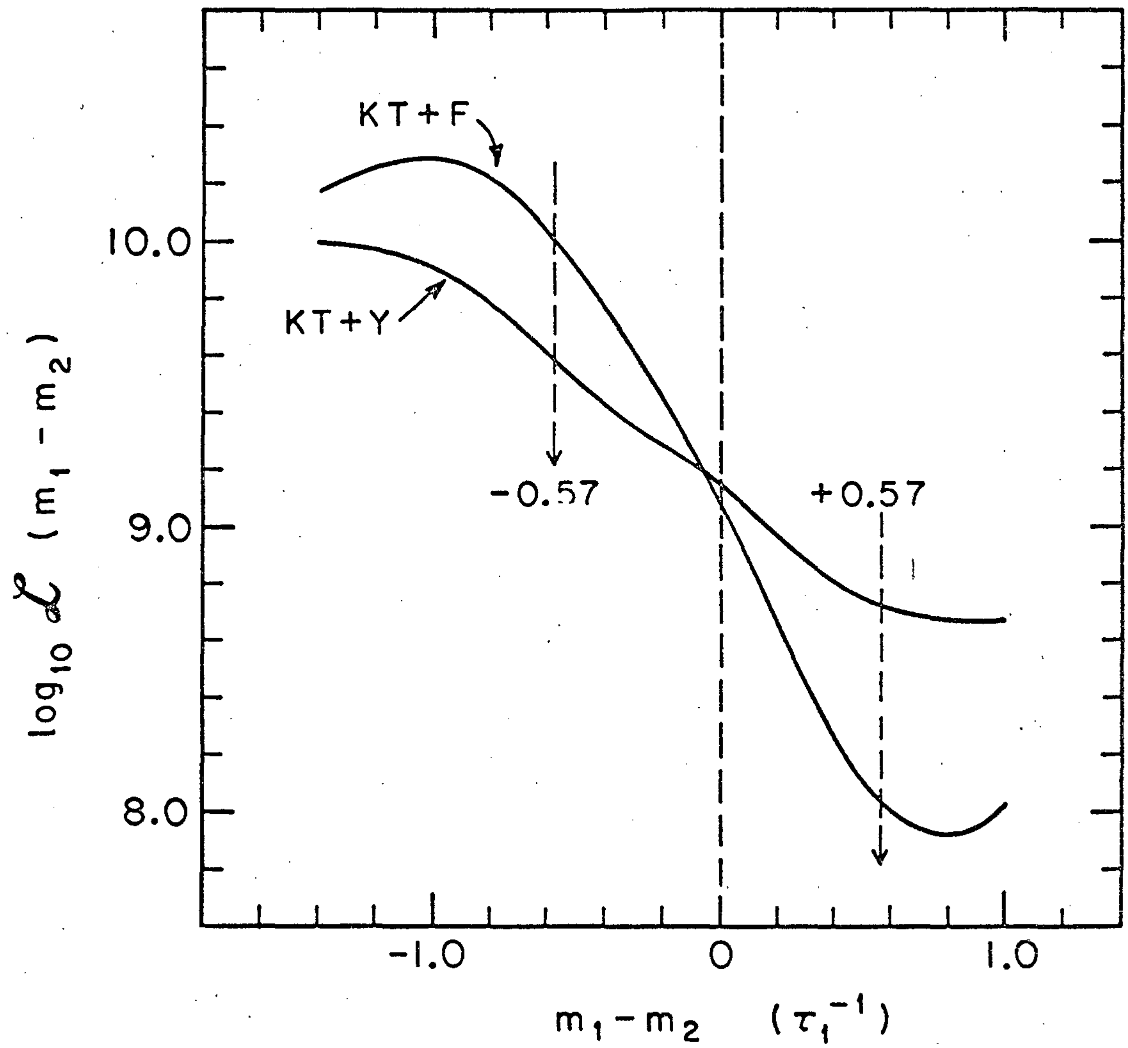

MUB-11393

Fig. 12. Likelihood function $\mathcal{L}(m_1-m_2)$ for 23 K_1^0 events.

is correct, then the most-probable value for $\log_{10} \mathcal{L}(+0.57)$ is 9.9 (10.2), and the probability of getting $\log_{10} \mathcal{L}(+0.57)$ as low or lower than our observed value of 8.72 is only 0.027 (0.001). Thus the fit is poor for the hypothesis $m_1 - m_2 = +0.57$.

We show the distribution of $\log_{10} \mathcal{L}(\pm 0.57)$ for solutions KT + Y and KT + F in Fig. 13.

Given the magnitude $\delta \equiv |m_1 - m_2|$, we summarize our data by giving the likelihood ratio $\mathcal{L}(-\delta) \equiv R(\delta)$, which is expected to be greater (less) than 1.0 for K_2^0 heavier (lighter) than K_1^0. For solutions KT + F and KT + Y, we obtain $R(0.57) = 95.1$ and 7.4, respectively. These likelihood ratios cannot be immediately interpreted as statistical "betting odds." To understand their statistical significance we again use the Monte Carlo method. For a given value of δ we generate 1000 MC experiments with the t_i chosen according to $m_1 - m_2 = +\delta$, and 1000 accord-to $m_1 - m_2 = -\delta$. Using the set of amplitudes KT + Y, we find that among the 1000 MC experiments generated assuming $m_1 - m_2 = -0.57$, there are five times as many experiments with $R(0.57) = 7.4$ (within a small interval ΔR) as there are experiments generated assuming $m_1 - m_2 = +0.57$. We therefore assign MC betting odds of 5 to 1 for K_2^0 heavier than K_1^0, assuming KT + Y. The corresponding MC betting odds involving KT + F are 45 to 1 for K_2 heavier than K_1. (We obtain essentially the same MC betting odds if we use the $S = -1$ solution KT' instead of KT.)

The distribution of $R(0.57)$ for solution KT + Y is shown in Fig. 14. In Fig. 15 we show betting odds (as determined by the above method) as a function of $|m_1 - m_2|$ for K_2^0 heavier than K_1^0 for several sets of scattering amplitudes.

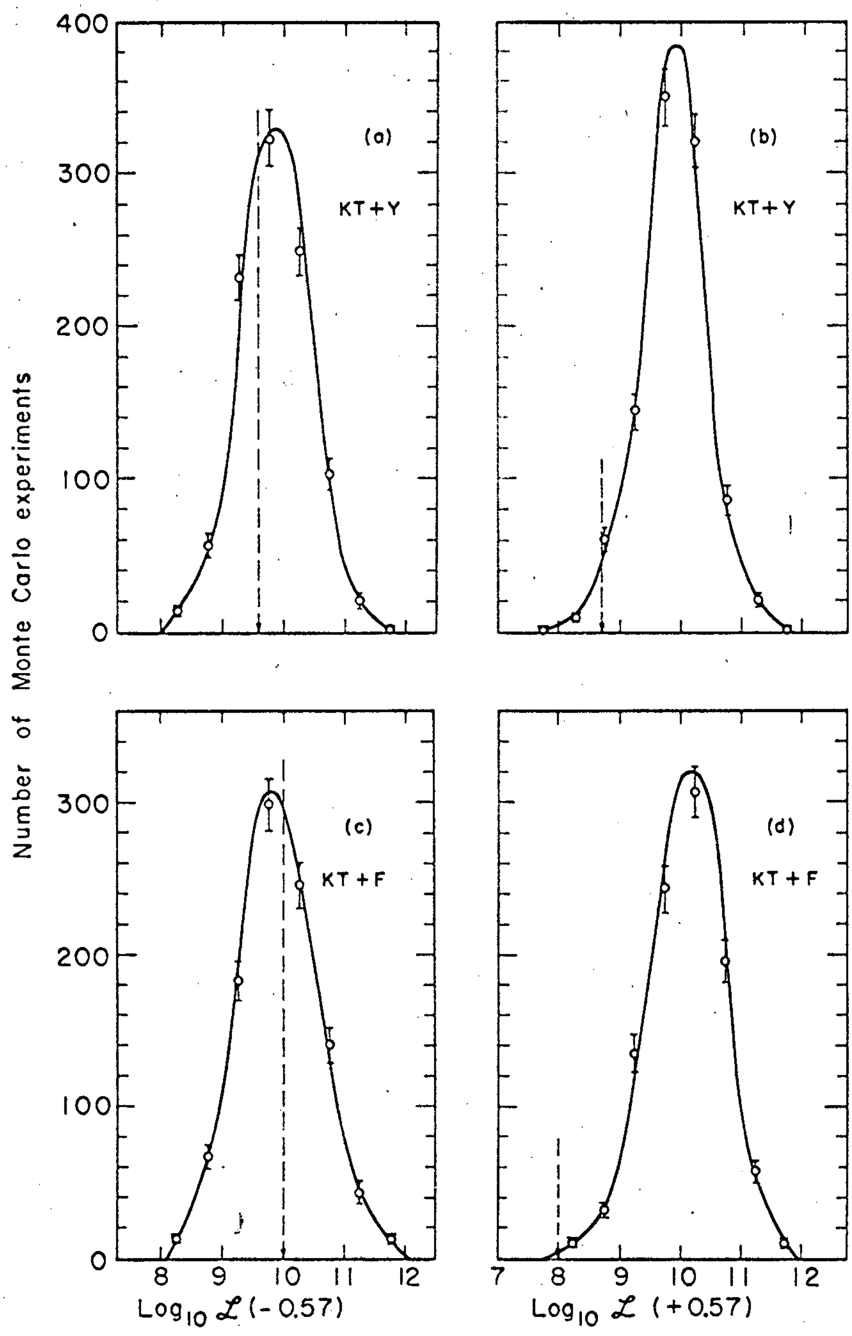

Fig. 13. Spectrum of $\log_{10}(m_1-m_2)$ from 1000 Monte Carlo experiments generated according to several sets of scattering amplitudes and values of m_1-m_2: (a) KT + Y, -0.57; (b) KT+ Y, +0.57; (c) KT + F, -0.57; (d) KT + F, +0.57.

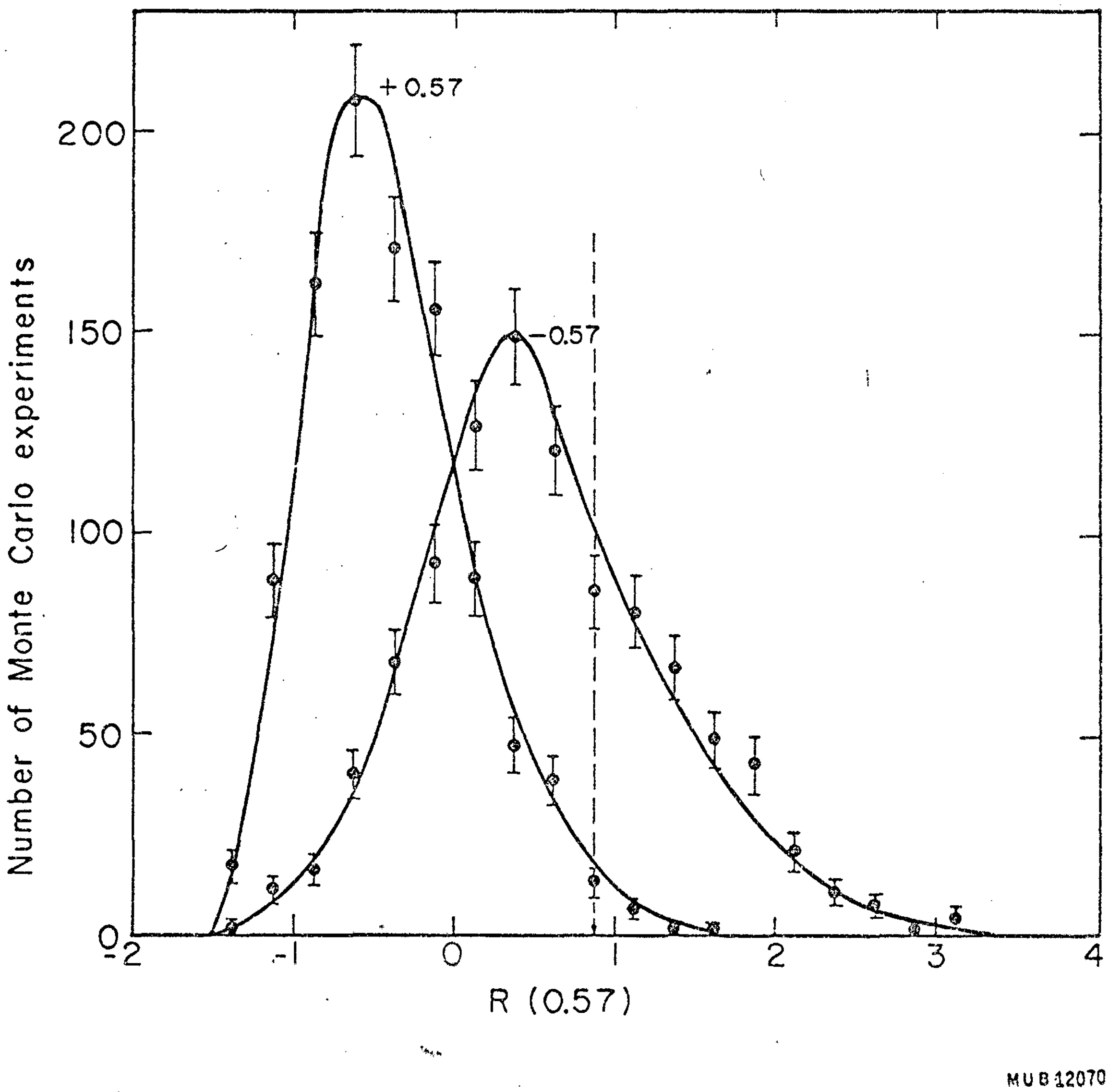

Fig. 14. Spectrum of R(0.57) from 1000 Monte Carlo experiments generated according to the hypothesis $m_1 - m_2 = \pm 0.57\ \tau_1^{-1}$ for solution KT + Y. Our experimental value of R(0.57) is indicated by the dashed line.

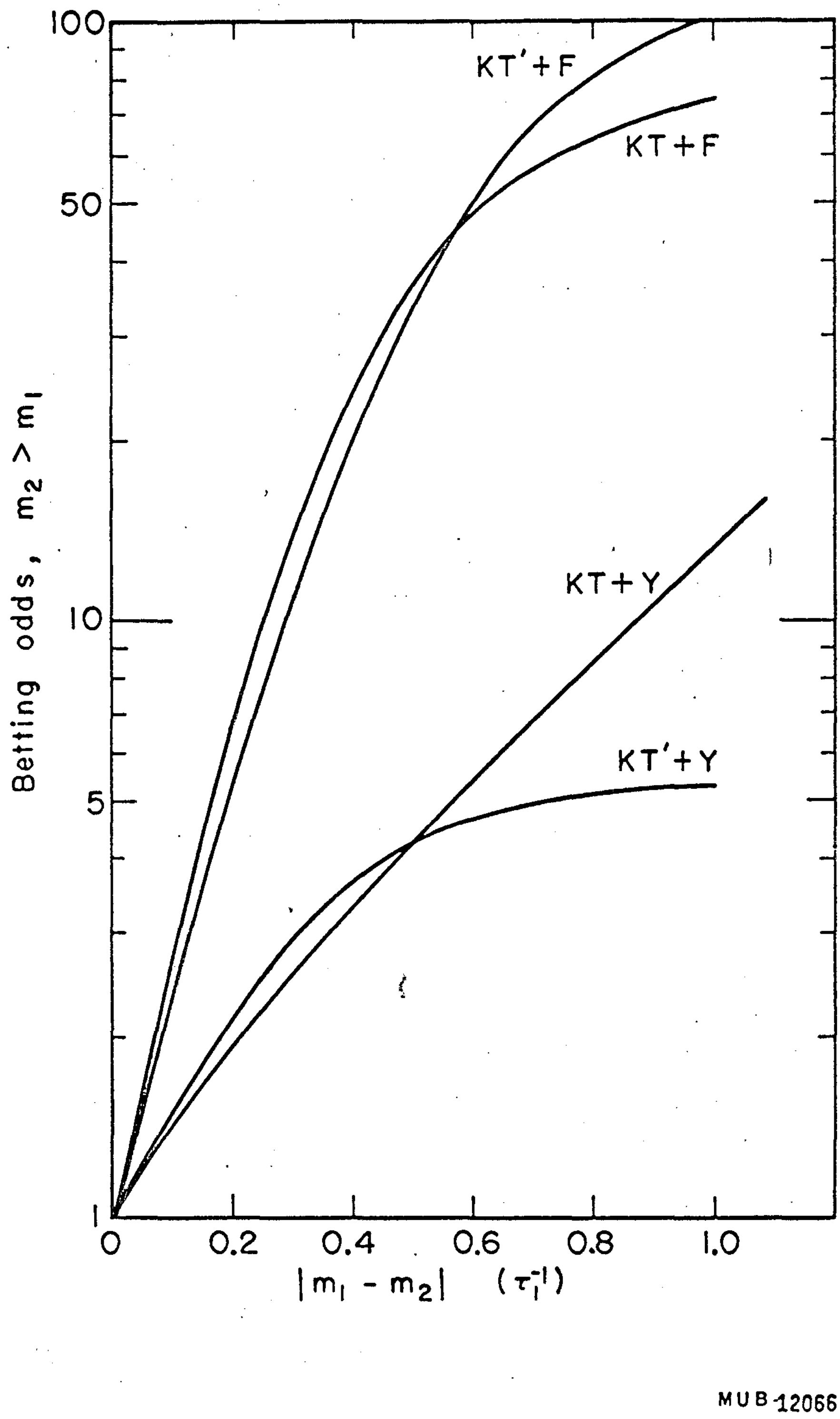

Fig. 15. Betting odds for K_2^0 heavier than K_1^0 as a function of $|m_1 - m_2|$ for several solutions of scattering amplitudes.

V. DISCUSSION

Our knowledge of KN and $\overline{K}N$ scattering amplitudes up to 600 MeV/c is not complete. In particular, we would like to resolve the Fermi-Yang-type ambiguity in the $I = 0$, KN channel in order to have a more complete knowledge of this system and definite betting odds for the sign of the mass difference (see Fig. 15).

To resolve the F-Y ambiguity requires looking at either K^+n or K^0p scattering. Measuring the polarization of the recoil proton in charge-exchange scattering of K^+ in deuterium or measuring the differential and total cross sections for the reaction $K_2^0 p \rightarrow K_1^0 p$ will suffice. Whereas the former method is beset with problems indigenous to deuterium, the latter method is applicable only if the $\overline{K}N$ amplitudes are well known, since the resolution of this ambiguity depends on the sensitivity of the cross sections to the $S = \pm 1$ interference terms. Film from an exposure of the 25-inch hydrogen bubble chamber at Berkeley to a K_2^0 beam with a momentum spread from 200 to 500 MeV/c is now being analyzed. Results from this experiment may resolve the Fermi-Yang ambiguity.

Degenerate second-order-perturbation calculations show that the sign of the $K_1^0 - K_2^0$ mass difference may indicate whether attractive 2π states lie above or below the K^0 mass. Some authors feel that the apparent magnitude and sign of the $K_1^0 - K_2^0$ mass difference along with the observed $K_1^0 \rightarrow 2\pi$ rate necessitates the existence of scalar mesons with a mass greater than that of the kaon.[33]

ACKNOWLEDGMENTS

I would like to thank Professor Frank S. Crawford, Jr., for his continual guidance throughout this experiment. His interest in and knowledge of many facets of physics is inspiring.

Thanks are also due Dr. Jared Anderson and Mr. Jack Lloyd, who helped build the beam and analysis system, and Dr. LeRoy Price, for numerous instructive discussions. Bevalyn B. Crawford wrote the bulk of the kinematic analysis routine and several other analysis programs. I am grateful to Dr. Robert L. Golden for his help during the early part of the experiment.

Because scanning and other human responsibilities were very essential to the success of this experiment, I want to specifically thank Arlene D. Bindloss, Edward A. Romascan, and Thomas H. Strong for their excellent work.

It is a pleasure to thank Professor Luis W. Alvarez for his interest and support.

This work was done under the auspices of the U. S. Atomic Energy Commission.

FOOTNOTES AND REFERENCES

1. We take $|m_1 - m_2| = 0.57\,\tau_1^{-1}$ (assuming $\tau_1 = 0.88\times10^{-10}$ sec) as an average of the results listed in Gerald W. Meisner, Bevalyn B. Crawford, and F. S. Crawford, Jr., Phys. Rev. Letters <u>16</u>, 278 (1966), plus the more recent results of C. Alff-Steinberger, W. Heurr, K. Kleinknecht, C. Rubbia, A. Scribano, J. Steinberger, M. J. Tannenbaum, and K. Tittel, Phys. Letters <u>20</u>, 207 (1966); of M. Bott-Bodenhausen, X. De Bonard, D. G. Cassel, D. Dekkers, R. Felst, R. Mermod, I. Savin, P. Scharff, M. Vivargent, T. R. Willitts, and K. Winter, Phys. Letters <u>20</u>, 212 (1966); and of R. March, U. Camerini, D. Cline, W. Fry, W. Fischbein, J. Gaidos, R. Hantman, and R. Stark, Bull. Am. Phys. Soc. <u>11</u>, 326 (1966).
2. Y. Kobzarov and L. B. Okun', Soviet Phys. JETP <u>12</u>, 426 (1961).
3. J. Jovanovich, T. Fujii, F. Turkot, G. T. Zorn, and M. Deutsch, Bull. Am. Phys. Soc. <u>11</u>, 469 (1966).
4. O. Piccioni et al., postdeadline paper GF16 at the 1966 Washington, D. C., meeting of the American Physical Society (unpublished).
5. U. Camerini, W. F. Fry, and J. Gaidos, Nuovo Cimento <u>28</u>, 1096 (1963). The recent discovery by J. H. Christenson, J. W. Cronin, V. L. Fitch, and R. Turlay, Phys. Rev. Letters <u>13</u>, 138 (1964), of the process $K_{long} \rightarrow \pi^+ + \pi^-$ has a negligible effect on the present experiment. We therefore use the old-fashioned notation K_1^0 and K_2^0 and neglect CP nonconservation.
6. A preliminary result was given by Gerald W. Meisner, Robert L. Golden, Bevalyn B. Crawford, and Frank S. Crawford, Jr., in <u>Proceedings of the International Conference on Fundamental Aspects of Weak Interactions</u>, Brookhaven National Laboratory Report BNL-837 (1963), p. 66 (unpublished), and in <u>Proceedings of the International Conference on Weak Interactions</u>, Argonne National Laboratory Report ANL-7130 (1965), p. 229 (unpublished).
7. The Yang-type phase shifts are favored by SU(3) invariance, according to Robert L. Warnock and Graham Frye, Phys. Rev. <u>138</u>, B947 (1965).

8. M. Gell-Mann and A. Pais, Phys. Rev. 97, 1387 (1955).
9. T. D. Lee, Reinhard Oehme, and C. N. Yang, Phys. Rev. 106, 340 (1957).
10. Frank S. Crawford, Jr., Roger L. Douglass, Myron L. Good, George R. Kalbfleisch, M. Lynn Stevenson, and Harold K. Ticho, Phys. Rev. Letters 3, 394 (1959).
11. V. F. Weisskopf and E. P. Wigner, Z. Physik 63, 54 (1930).
12. The corrections to Eqs.(3) and (4) due to coherent regeneration in liquid hydrogen is negligible.
13. See, for example, Robert A. Becker, Introduction to Theoretical Mechanics (McGraw-Hill, New York, 1954), Chap. 14.
14. This factorization is possible at low energy where only S-wave contributes, since there generally is a non-spin-flip and a spin-flip amplitude which are orthogonal to each other.
15. Sanford E. Wolf, Norbert Schmitz, Lester J. Lloyd, William Laskar, Frank S. Crawford, Jr., Janice Button, Jared A. Anderson, and Gideon Alexander, Rev. Mod. Phys. 33, 439 (1961).
16. See, for example, William E. Humphrey and Arthur H. Rosenfeld, Ann. Rev. Nucl. Sci. 13, 103 (1963).
17. M. H. Alston, J. E. Braley, and P. White, QUEST—An On-Line Event-Processing Routine, UCRL-10501, August 8, 1962; also M. H. Alston, J. E. Braley, J. Stedman, M. L. Stevenson, and P. White, QUEST Operating Manual, Alvarez Group Memo No. 543, May 30, 1963.
18. Frank S. Crawford, Jr., Phys. Rev. Letters 15, 1045 (1965).
19. When, for part of the film, the azimuthal width of the scanned region was doubled to ±10 deg and the K^0- direction criterion relaxed to seven standard deviations, no new good candidates were found.
20. Sulamith Goldhaber, William Chinowsky, Gerson Goldhaber, Wonyong Lee, Thomas O'Halloran, Theodore F. Stubbs, Phys. Rev. Letters 9, 135 (1962).
21. D. Keefe, A. Kernan, A. Montwill, M. Grilli, L. Guerriero, and G. A. Salandin, Nuovo Cimento 12, 241 (1959).

22. T. F. Kycia, L. T. Kerth, and R. G. Baender, Phys. Rev. 118, 553 (1960).

23. William Slater, Donald Stork, Harold K. Ticho, Wonyong Lee, William Chinowsky, Gerson Goldhaber, Sulamith Goldhaber, and Thomas O'Halloran, Phys. Rev. Letters 7, 378 (1961).

24. V. J. Stenger, W. E. Slater, D. H. Stork, H. K. Ticho, G. Goldhaber, and S. Goldhaber, Phys. Rev. 134, B1111 (1964).

25. William E. Humphrey and Ronald R. Ross, Phys. Rev. 127, 1305 (1962).

26. Jae Kwan Kim, Phys. Rev. Letters 14, 29 (1965).

27. M. Sakitt, T. B. Day, R. G. Glasser, N. Seeman, J. Friedman, W. E. Humphrey, and R. R. Ross, Phys. Rev. 139, 712 (1965).

28. Mason B. Watson, Massimiliano Ferro-Luzzi, and Robert D. Tripp, Phys. Rev. 131, 2248 (1963).

29. J. A. Kadyk, T. Oren, R. Brower, J. L. Brown, I. Butterworth, G. Goldhaber, S. Goldhaber, J. McNaughton, B. C. Shen, and G. H. Trilling, Bull. Am. Phys. Soc. 11, 37 (1966); John Kadyk, Invited Paper HC2, Bull. Am. Phys. Soc. 11, 380 (1966).

30. Nripendra N. Biswas, Phys. Rev. 118, 866 (1960).

31. The mass of the $Y^*_1(1385)$ is below threshold; however, the energy dependence of the width and angular momentum barriers result in a non-negligible contribution to the $\bar{K}N$ $p_{3/2}$ partial-wave amplitude at our momenta. This amplitude must have a negative real part, in agreement with the $p_{3/2}$ amplitude for solution KT'.

32. Even if we had very many events with known k_i and θ_i but not t_i, we would have essentially no information useful for finding the sign of $m_1 - m_2$. Therefore, we do not generate random values of k_i and θ_i in the MC experiments, but instead confine ourselves to generating t_i, thus avoiding irrelevant fluctuations that would arise from MC-generated k_i and θ_i.

33. D. Loebbaka, S. Oneda, and J. C. Pati, Normal Scalar Nonet; $K_1 \rightarrow 2\pi$-Decay and $K_1 - K_2$ Mass Difference, Technical Report No. 511, University of Maryland, October 1965.